Optimal Frequency-Domain System Realization with Weighting

Jer-Nan Juang and Peiman G. Maghami
Langley Research Center, Hampton, Virginia

April 1999

Optimal Frequency-Domain System Realization with Weighting

Jer-Nan Juang and Peiman G. Maghami
Langley Research Center, Hampton, Virginia

Optimal Frequency-Domain System Realization with Weighting

Jer-Nan Juang *and Peiman G. Maghami †

NASA Langley Research Center

Hampton, VA 23681

Abstract

Several approaches are presented to identify an experimental system model directly from frequency response data. The formulation uses a matrix-fraction description as the model structure. Frequency weighting such as exponential weighting is introduced to solve a weighted least-squares problem to obtain the coefficient matrices for the matrix-fraction description. A multi-variable state-space model can then be formed using the coefficient matrices of the matrix-fraction description. Three different approaches are introduced to fine-tune the model using nonlinear programming methods to minimize the desired cost function. The first method uses an eigenvalue assignment technique to reassign a subset of system poles to improve the identified model. The second method deals with the model in the real Schur or modal form, reassigns a subset of system poles, and adjusts the columns (rows) of the input (output) influence matrix using a nonlinear optimizer. The third method also optimizes a subset of poles, but the input and output influence matrices are refined at every optimization step through least-squares procedures.

1 Introduction

One major objective of system identification is to provide mathematical models for dynamics and control analysis and designs. However, models of systems can have

---

*Principal Scientist, Structural Dynamics Branch, (j.juang@larc.nasa.gov)

†Senior Aerospace Engineer, Guidance and Control Branch, (p.g.maghami@larc.nasa.gov)

various forms, such as transfer functions, differential or difference equations, and state-space equations. A frequency-domain state-space identification method [1 − 5] provides a state-space model of a linear system from frequency response data.

The method called the State-Space Frequency Domain (SSFD) identification algorithm [2] can estimate Markov parameters (pulse response) from the frequency response function (FRF) without window distortion when an arbitrary frequency weighting is used to shape the estimation error. The method uses a rational matrix fraction description (the ratio of a matrix polynomial and a monic scalar polynomial denominator) to curve-fit the frequency data and compute the Markov parameters from FRF. The curve-fitting problem must be solved either by nonlinear optimization techniques or by linear approximate algorithms with several iterations. To obtain the state-space models from the Markov parameters, the Eigensystem Realization Algorithm (ERA) or its variant ERA/DC is used [5].

Frequency domain methods presented in Refs. [3, 4, 5] start with identifying a left matrix-fraction description (LMFD) of the transfer function matrix. The advantage of using the LMFD, as an intermediate model between the data and the desired final state-space model, is that from frequency response data to the LMFD is a linear least-squares problem, which is easy to solve. This method works quite well when the frequency response data are fairly accurate; however, it might yield unstable, erroneous models if the data contains too much distortion and/or error. Data distortion in the frequency domain is caused by a number of factors; limited sampling frequency, filters to remove noise, and lack of periodicity. This data distortion often cause unstable modes to be present in the identified system model. An improved method was introduced in Ref. [6] to deal with the problem when data distortion is present. The idea is to stabilize or remove the unstable modes before expanding the matrix-fraction description (MFD) into the Markov parameters (pulse responses). This approach avoids introducing unstable modes while still maintaining the frequency response close to the data.

In this paper, exponential frequency weighting [2, 7] is used to solve a weighted least-squares problem for the LMFD coefficient matrices. A multi-variable state-space

2

model is then realized from the LMFD coefficient matrices. To improve the identified model, nonlinear programming methods [8] are used to fine-tune the model parameters. There are three different formulations introduced in this paper for parameter optimization. In all three formulations, the objective function is defined as the error between the actual FRF and the synthesized FRF using the identified space-space model. The first formulation uses a general system realization, and utilizes nonlinear programming along with an eigenvalue assignment [9 − 11] technique to optimize a subset of system poles. The second formulation deals with system realizations in the real Schur or modal forms, and uses a subset of system poles, as well as some coefficients to adjust the columns (rows) of the input (output) influence matrix for parameter optimization. The third formulation is similar to the second, but the input and output influence matrices are computed at every optimization step through least-squares procedures. Experimental data from a NASA testbed with fifteen inputs and fourteen outputs are used with a total of two hundreds and ten transfer functions to demonstrate the concepts proposed in this paper.

2 Weighted Least-Squares Method

Given the system frequency response function $G(z_k)$ at the frequency point z_k, consider the left matrix-fraction

$$G(z_k) = \alpha^{-1}(z_k)\beta(z_k) \tag{1}$$

where
$$\alpha(z_k) = I_m + \alpha_1 z_k^{-1} + \cdots + \alpha_p z_k^{-p} \tag{2}$$

$$\beta(z_k) = \beta_0 + \beta_1 z_k^{-1} + \cdots + \beta_p z_k^{-p} \tag{3}$$

are matrix polynomials with I_m being an identity matrix of order m. Every α_i is an $m \times m$ real square matrix and each β_i is an $m \times r$ real rectangular matrix. The factorization in Eq. (1) is not unique. For convenience and simplicity, one can choose the orders of both polynomials to be equal to p.

3

Pre-multiplying Eq. (1) by $\alpha(z_k)$ produces

$$\alpha(z_k)G(z_k) = \beta(z_k) \tag{4}$$

which can be rearranged into

$$\begin{aligned} G(z_k) &= -\alpha_1 G(z_k)z_k^{-1} - \cdots - \alpha_p G(z_k)z_k^{-p} \\ &\quad + \beta_0 + \beta_1 z_k^{-1} + \cdots + \beta_p z_k^{-p} \end{aligned} \tag{5}$$

or

$$G(z_k) = \Theta \mathcal{G}_k \tag{6}$$

where the matrix Θ, of dimension $m \times [p(m+r)+r]$, and the matrix $\mathcal{G}_k$, of dimension $[p(m+r)+r] \times r$, are defined as

$$\Theta = \begin{bmatrix} \alpha_1 & \cdots & \alpha_p & \beta_0 & \beta_1 & \beta_2 & \cdots & \beta_p \end{bmatrix} \tag{7}$$

$$\mathcal{G}_k = \begin{bmatrix} G(z_k)z_k^{-1} \\ \vdots \\ G(z_k)z_k^{-p} \\ I_r \\ I_r z_k^{-1} \\ \cdots \\ I_r z_k^{-p} \end{bmatrix} \tag{8}$$

Here, I_r is an $r \times r$ identity matrix. With $G(z_k)$ and z_k^{-1} known, Eq. (5) or (6) is a linear equation. Because $G(z_k)$ is known at $z_k = e^{j\frac{2\pi(k-1)}{\ell}}$ $(k = 1, \ldots, \ell)$, there are ℓ equations available.

The parameter matrix Θ in Eq. (6) is a real matrix whereas $G(z_k)$ and $\mathcal{G}_k$ are both complex matrices. Thus Eq. (6) is a complex matrix equation with a total of ℓ complex equations . Let us define

$$\tilde{G}_k = [\text{Real}(G(z_k)) \ \text{Imag}(G(z_k))] \quad \text{and} \quad \tilde{\mathcal{G}}_k = [\text{Real}(\mathcal{G}_k) \ \text{Imag}(\mathcal{G}_k)] \tag{9}$$

4

Equation (6) may be rewritten as

$$\tilde{G}_k = \Theta \tilde{\mathcal{G}}_k \tag{10}$$

Equation (10) is a real matrix equation consisting of 2ℓ linear equations for computing the parameter matrix Θ. The matrix $\tilde{G}_k$ at the frequency point k is an $m \times 2r$ matrix, whereas $\tilde{\mathcal{G}}_k$ is a $[p(m + r) + r] \times 2r$ matrix.

2.1 Recursive Formulation

To solve Eq. (10), let us first define a weighted cost function to be minimized as

$$J(\Theta, k) = \sum_{i=1}^{k} w^{k-i} \parallel \Theta(k)\tilde{\mathcal{G}}_{\ell-i} - \tilde{G}_{\ell-i} \parallel_2^2 \tag{11}$$

where $0 < w \leq 1$ is a forgetting factor weighting the frequency data. The data at the lowest frequency point is given unit weight, but data that is k frequency points higher is weighted by w^k. The method is commonly called exponential forgetting. The cost function defined in Eq. (11) is motivated by the fact that accelerometers are commonly used as the measurement device in structural testing. The corresponding frequency response functions have better response levels in the high frequency range. Identifying lower frequency information in the presence of measurement noise becomes a problem. One way to solve this problem is to weight more the lower frequency region. On the other hand, displacement sensors have better response capability for the low frequency region. For this case, the forgetting factor may be switched to weight the high frequency region more than the lower frequency region. The form of Eq. (11) is unchanged except for the index $\ell - i$ is replaced by i.

Using recursive least squares, the solution that minimizes Eq. (11) is

$$\Theta(k) = \phi(k)P(k) \tag{12}$$

where

$$\phi(k) = \sum_{i=1}^{k} w^{k-i}\tilde{G}_{\ell-i}\tilde{\mathcal{G}}_{\ell-i}^T \tag{13}$$

$$P(k) = \left[\sum_{i=1}^{k} w^{k-i}\tilde{\mathcal{G}}_{\ell-i}\tilde{\mathcal{G}}_{\ell-i}^T \right]^{-1} \tag{14}$$

5

The matrix $P(k)$ is the inverse of the frequency data correlation matrix weighted by the forgetting factor w. Note that the matrix $P(k)$ is positive definite. From the definition of $P(k)$, application of the matrix inversion lemma yields

$$
\begin{aligned}
P(k) &= \left[\sum_{i=1}^{k} w^{k-i} \tilde{\mathcal{G}}_{\ell-i} \tilde{\mathcal{G}}_{\ell-i}^T \right]^{-1} \\
&= \left[w \left(\sum_{i=1}^{k-1} w^{k-1-i} \tilde{\mathcal{G}}_{\ell-i} \tilde{\mathcal{G}}_{\ell-i}^T \right) + \tilde{\mathcal{G}}_{\ell-k} \tilde{\mathcal{G}}_{\ell-k}^T \right]^{-1} \\
&= \left[w P^{-1}(k-1) + \tilde{\mathcal{G}}_{\ell-k} \tilde{\mathcal{G}}_{\ell-k}^T \right]^{-1} \\
&= \frac{1}{w} P(k-1) - \frac{1}{w} P(k-1) \tilde{\mathcal{G}}_{\ell-k} \mathcal{K}(k-1)
\end{aligned}
\tag{15}
$$

where

$$
\mathcal{K}(k-1) = [w I_{2r} + \tilde{\mathcal{G}}_{\ell-k}^T P(k-1) \tilde{\mathcal{G}}_{\ell-k}]^{-1} \tilde{\mathcal{G}}_{\ell-k}^T P(k-1)
\tag{16}
$$

Similarly, the quantity $\phi(k+1)$ at frequency point $k+1$ can be written as

$$
\begin{aligned}
\phi(k) &= \sum_{i=1}^{k} w^{k+1-i} \tilde{G}_{\ell-i} \tilde{\mathcal{G}}_{\ell-i}^T \\
&= w \phi(k-1) + \tilde{G}_{\ell-k} \tilde{\mathcal{G}}_{\ell-k}^T
\end{aligned}
\tag{17}
$$

Substituting Eqs. (15) and (16) into Eq. (12) yield the parameter $\Theta(k)$

$$
\begin{aligned}
\Theta(k) &= \phi(k) P(k) \\
&= \left[w \phi(k-1) + \tilde{G}_{\ell-k} \tilde{\mathcal{G}}_{\ell-k}^T \right] \left[\frac{1}{w} P(k-1) - \frac{1}{w} P(k-1) \tilde{\mathcal{G}}_{\ell-k} \mathcal{K}(k-1) \right] \\
&= \Theta(k-1) + \left[\tilde{G}_{\ell-k} - \Theta(k-1) \tilde{\mathcal{G}}_{\ell-k} \right] \mathcal{K}(k-1)
\end{aligned}
\tag{18}
$$

where the last equality results from the following

$$
\begin{aligned}
&\tilde{\mathcal{G}}_{\ell-k}^T \left[\frac{1}{w} P(k-1) - \frac{1}{w} P(k-1) \tilde{\mathcal{G}}_{\ell-k} \mathcal{K}(k-1) \right] \\
&= \frac{1}{w} \left\{ [w I_{2r} + \tilde{\mathcal{G}}_{\ell-k}^T P(k-1) \tilde{\mathcal{G}}_{\ell-k}] - \tilde{\mathcal{G}}_{\ell-k}^T P(k-1) \tilde{\mathcal{G}}_{\ell-k} \right\} \mathcal{K}(k-1) \\
&= \mathcal{K}(k-1)
\end{aligned}
\tag{19}
$$

6

The parameter $\Theta(k)$ which minimizes the cost function is given recursively by

$$\tilde{G}_{\ell-k} = [\text{Real}(G(z_{\ell-k}))\ \text{Imag}(G(z_{\ell-k}))]$$

$$\mathcal{G}_k = \begin{bmatrix} G(z_{\ell-k})z_{\ell-k}^{-1} \\ \vdots \\ G(z_{\ell-k})z_{\ell-k}^{-p} \\ I_r \\ I_r z_{\ell-k}^{-1} \\ \cdots \\ I_r z_{\ell-k}^{-p} \end{bmatrix} ; \quad z_{\ell-k} = e^{j\frac{2\pi(\ell-k-1)}{\ell}}$$

$$\tilde{\mathcal{G}}_{\ell-k} = [\text{Real}(\mathcal{G}_{\ell-k})\ \text{Imag}(\mathcal{G}_{\ell-k})]$$

$$\mathcal{K}(k-1) = [wI_{2r} + \tilde{\mathcal{G}}_{\ell-k}^T P(k-1)\tilde{\mathcal{G}}_{\ell-k}]^{-1}\tilde{\mathcal{G}}_{\ell-k}^T P(k-1)$$

$$\hat{G}_{\ell-k} = \Theta(k-1)\tilde{\mathcal{G}}_{\ell-k}$$

$$P(k) = \frac{1}{w}P(k-1) - \frac{1}{w}P(k-1)\tilde{\mathcal{G}}_{\ell-k}\mathcal{K}(k-1)$$

$$\Theta(k) = \Theta(k-1) + \left[\tilde{G}_{\ell-k} - \hat{G}_{\ell-k}\right]\mathcal{K}(k-1)$$

At any specific frequency point k, the $m \times 2r$ FRF matrix $\tilde{G}_{\ell-k}$ is given, where r is the number of inputs, m is the number of outputs, and ℓ is the total number of frequency points to be used for the identification process. The $[p(r+m)+r] \times r$ complex matrix $\mathcal{G}_k$ is then computed where p is an integer large enough to satisfy the constraint $pm \geq n$ (the system order). The $2r \times [p(r+m)+r]$ matrix $\mathcal{K}(k-1)$ is the update gain determined by the matrix $P(k-1)$ of dimension $[p(r+m)+r] \times [p(r+m)+r]$, the matrix $\tilde{\mathcal{G}}_{\ell-k}$ of dimension $[p(r+m)+r] \times 2r$, and the scalar w. The initial values of $P(0)$ and $\Theta(0)$ can be arbitrarily assigned. normally, $P(0)$ and $\Theta(0)$ are assigned as dI and 0, respectively, where d is a large positive number, I is an identity matrix dimensioned $[p(r+m)+r] \times [p(r+m)+r]$, and 0 is a zero matrix dimensioned $m \times [p(r+m)+r]$.

In the recursive process, special care must be taken to ensure that both matrices

7

$[wI_{2r} + \tilde{\mathcal{G}}_{\ell-k}^T P(k-1)\tilde{\mathcal{G}}_{\ell-k}]^{-1}$ and $P(k)$ must be symmetric and positive definite. In theory, inverting a positive-definite matrix results in another positive-definite matrix. In practice, any numerical error in the matrix inversion process at any step may accumulate large enough errors to destroy its symmetry and positive-definiteness. It eventually leads to an unstable solution, i.e., the parameter Θ will not converge to a constant value when $k \to \ell$. One simple way to eliminate the inversion problem is to take only the symmetric part of the inverted matrix at every recursion step, i.e., $\frac{1}{2}\{[wI_{2r} + \tilde{\mathcal{G}}_{\ell-k}^T P(k-1)\tilde{\mathcal{G}}_{\ell-k}]^{-1} + ([wI_{2r} + \tilde{\mathcal{G}}_{\ell-k}^T P(k-1)\tilde{\mathcal{G}}_{\ell-k}]^{-1})^T\}$. This will guarantee that the inverted matrix is symmetric.

2.2 Batch Formulation

Recursive approaches are better suited for computations in real time, i.e., parameters are computed as data becomes available. Often, experimental data from a completed test is available which allows all calculations to be performed at once. A batch version is presented in this section. Stacking up the 2ℓ equations in Eq. (10) yields

$$\tilde{G} = \Theta\tilde{\mathcal{G}} \tag{20}$$

where

$$\begin{aligned} \tilde{G} &= \begin{bmatrix} \tilde{G}_0 & \tilde{G}_1 & \cdots & \tilde{G}_\ell \end{bmatrix} \\ \tilde{\mathcal{G}} &= \begin{bmatrix} \tilde{\mathcal{G}}_0 & \tilde{\mathcal{G}}_1 & \cdots & \tilde{\mathcal{G}}_\ell \end{bmatrix} \end{aligned} \tag{21}$$

The cost function J shown in Eq. (11) is minimized by solving the least-squares solution for Θ according to Eqs. (12), (13), (14) with $k = \ell$,

$$\Theta = \tilde{G}\tilde{\mathcal{G}}_w^T[\tilde{\mathcal{G}}\tilde{\mathcal{G}}_w^T]^{-1} \tag{22}$$

where

$$\tilde{\mathcal{G}}_w = \begin{bmatrix} \tilde{\mathcal{G}}_0 & w\tilde{\mathcal{G}}_1 & \cdots & w^\ell\tilde{\mathcal{G}}_\ell \end{bmatrix} \tag{23}$$

The subscript w associated with $\tilde{\mathcal{G}}_w$ signifies the forgetting factor w inserted into $\tilde{\mathcal{G}}$ with an appropriate power at each frequency point.

The weighting w^ℓ for the highest frequency at the frequency point ℓ can be quite small depending on the length ℓ of the data and the choice of the forgetting factor w.

Fox example, $w^\ell \approx 4.3 \times 10^{-5}$ with $\ell = 1000$ and $w = 0.99$. Unless the amplitudes of those frequencies near the highest frequency are in the order of 10^{-5}, their contribution to the identification process may become negligible. Using accelerometers, the ratio of the highest frequency to the lowest frequency can be as high as 10^3 to 10^5. For this case, the forgetting factor used in Eq. (23) is indeed a good weighting technique to perform a better low-frequency identification.

On the other hand, one may prefer to have freedom of choosing a weighting factor. A slight modification of Eq. (23) will provide such freedom, i.e.,

$$\tilde{\mathcal{G}}_w = \begin{bmatrix} \tilde{\mathcal{G}}_0 & w_1\tilde{\mathcal{G}}_1 & \cdots & w_\ell\tilde{\mathcal{G}}_\ell \end{bmatrix} \tag{24}$$

The quantities $w_1, w_2, \ldots, w_\ell$, can be all independent. They may be randomly or specifically chosen. Some obvious choices include

$$w_k = e^{-10(1-k)/\ell}, \quad w_k = \frac{1}{k}, \quad w_k = \frac{1}{k^2}; \quad k = 1, 2, \ldots, \ell$$

For the case where the low frequency resolution is better than the high frequency resolution, the weighting must be reversed.

Substituting Eq. (24) in Eq. (22) and solving for the parameter Θ that minimizes the following cost function,

$$J(\Theta, \ell) = \sum_{i=1}^{\ell} w_i \parallel \Theta\tilde{\mathcal{G}}_i - \tilde{G}_i \parallel_2^2 \tag{25}$$

yields results similar to Eq. (11) except for the weighting factor.

In the next section, optimization-based approaches to further improve the least-square solution are discussed.

3 Nonlinear Optimization

Another approach to enhance the identified model is to use nonlinear programming to tune the model parameters obtained from the solution to Eq. (10). Once the solution, represented by the parameter matrix Θ, is computed using Eq. (18) or

9

Eq. (22), a state-space realization is determined. The state-space realization can be in any canonical form such as Schur form, modal form, Jordan form, observable form, etc. There are three different formulations considered in this paper for parameter optimization. The first formulation deals with a general system realization, and utilizes nonlinear programming along with an eigenvalue assignment technique to optimize a subset of system poles to improve the agreement between the measured transfer function and the identified model. The second formulation deals with system realizations in the real Schur or modal forms, and uses a subset of system poles, as well as some newly defined parameters to adjust the columns (rows) of the input (output) influence matrix, as optimization parameters. The third formulation is similar to the second, but the input and output influence matrices are not directly adjusted by the optimizer, rather, they are computed at every optimization step through least-squares procedures. In the first formulation, all system poles are reassigned simultaneously to the desired values given by the optimizer, via an eigenvalue assignment technique. In the second and third approaches , each pole is individually reassigned by the optimizer.

3.1 Parameter optimization: Eigenvalue Assignment

In this formulation, a subset of system poles are used as optimization parameters to minimize a cost function, which measures the difference between the experimental transfer function and the identified transfer function over frequency range of interest. Of course, the direct approach would be to use the elements of the state matrix directly, with equality constraints to reassign the poles. However, this approach is computationally expensive since it requires too many design parameters. Let (A_0, B, C, D) represent an initial realization for the identified system. As mentioned earlier, to determine the changes in the state matrix, A_0, which reflects the new pole locations (as defined by the optimization), an eigenvalue assignment technique is employed. Specifically, the eigenvalue assignment technique discussed in Ref. [10] is used, which is a sequential algorithm well-suited for partial assignment of eigenvalues in large-order systems.

10

Assume that the optimizer requires a subset of system poles to be reassigned to λ_d. Now, consider a system $(A_0, \tilde{B})$, where $\tilde{B}$ is an $n \times r$ random matrix representing an arbitrary input influence matrix. The matrix $\tilde{B}$ can have as many columns one would like, however, a reasonable choice would be $max(m, r)$. The change in the state matrix that would reassign the poles to λ_d is given by the gain matrix F such that the eigenvalues of $A_0 - \tilde{B}F$ are assigned to λ_d. Since the matrix $\tilde{B}$ has typically more than one column, the gain matrix F is not unique, i.e., there is freedom beyond eigenvalue assignment. This freedom is used to minimize the norm of the gain matrix, and hence, the effective changes in the state matrix. The reader is referred to Ref. [10] for a detailed description of the eigenvalue assignment algorithm. Once the gain matrix F is computed, the new system realization is given by $(A_0 - \tilde{B}F, B, C, D)$, i.e.,

$$\hat{G}(z_k) = C(z_k I_n - A_0 + \tilde{B}F)^{-1}B + D \tag{26}$$

In the next section, an optimization problem is posed for this approach.

3.1.1 Absolute Error Cost Function

Using a measure of the absolute error as the cost function, the optimization problem for system identification enhancement is defined as follows:

minimize J:

$$J = \|G(z_k) - \hat{G}(z_k)\|_F \tag{27}$$

over

$$\lambda_s$$

subject to

$$|\lambda_s| < 1$$

Here, λ_s represents a subset of the poles of the identified system $\hat{G}(z_k)$ which are used as design parameters, and $|\ |_F$ denotes the Frobenius norm. The constraint on the modulus of λ_s guarantees the stability of the identified system, and can be omitted if stability is not of concern. The computational procedure is as follows:

1. Compute new pole locations, λ_s using optimizer.

11

2. Determine the new state matrix, with eigenvalues at λ_s, using the sequential eigenvalue assignment technique described in Ref. [10].

3. Update the identified transfer function matrix $\widehat{G}(z_k)$ from Eq. (26), and compute the cost function J from Eq. (27).

The number of poles that can be used as design parameters in the optimization is arbitrary. One can use all the poles in the system, or just a few, for example, the real poles of the system. If one starts the optimization with a system realization from the least-squares solution of Eq. (13), then it is very likely that the complex poles of the identified system, representing resonant peaks in the frequency response plots, match the experimental results well, and hence need not be manipulated any further. In such a case, real poles of the system and unstable poles, real or complex, are the best candidates for design optimization. However, one could conceivably use the modulus of all complex poles, which determine the damping associated with each mode, as design parameters as well.

One of the problems with nonlinear programming is the tendency of the solution to converge to a local minimum. The problem becomes more aggravated as the number of design parameters increases. One way to deal with this problem is to restart the optimization from another set of design points in the neighborhood of the last optimal design. Another way of avoiding this problem is to introduce an additional constraint requiring that the cost function be less than a desired value, i.e.,

$$J \leq J_d \tag{28}$$

This constraint would move many of the local minima to the infeasible region, thereby avoiding them. An additional technique for dealing with local minima, which is more specific to the optimization problem that is being solved, is to restart the optimization of Eq. (27) with a new fictitious input influence matrix. Let $\tilde{B}_1$ represent the first input influence matrix, then choose the second influence matrix $\tilde{B}_2$ randomly from the null space of $\tilde{B}_1$, i.e.,

$$\tilde{B}_2 = N_{\tilde{B}_1} R_1 \tag{29}$$

12

where $N_{\tilde{B}_1}^T \tilde{B}_1 = 0$, and R_1 is a random matrix of appropriate dimensions. The transfer function of the system is then computed as

$$\hat{G}(z_k) = C(z_k I_n - A_1 + \tilde{B}_2 F_2)^{-1}B + D \qquad (30)$$

with

$$A_1 = A_0 - \tilde{B}_1 F_1$$

Now, the optimization of Eq. (27) is restarted with $\tilde{B}_2$ as the input influence matrix. This process can be continued until either an acceptable cost function is achieved or the computational burden of optimization outweighs any reductions in the cost function.

The cost function in Eq. (27), which is the Frobenius norm of the error in the transfer functions (experimental and identified), is dominated by the peaks (resonants) of the transfer functions. Hence, optimization with Eq. (27) works well in reducing the errors at or around those peaks, or wherever the transfer function magnitude is significant, but it may not do much in reducing the errors elsewhere, e.g., zeros. In fact, the errors around the valleys might become worst. An approach to deal with this problem is presented next.

3.1.2 Relative Error Cost Function

A more equitable trade between the errors for peaks and valleys can be obtained by considering a complementary optimization problem, wherein a norm of the relative error is optimized instead of the absolute error given in Eq. (27). The optimization problem is posed as

minimize J_2:

$$J_2 = ||[G(z_k) - \hat{G}(z_k)]./G(z_k)||_F \qquad (31)$$

over

$$\lambda_s$$

subject to

$$J \leq J_d$$

$$|\lambda_s| < 1$$

Here, J is the Frobenius norm of the absolute error given by Eq. (27) and "./" denotes element by element division. The upper bound limit J_d can be any desired value, but might be set at the optimal value of J, using a previously computed value from Eq. (27), or might be set at the value of J from an initial least-squares solution. Similarly, the initial values of the design parameters may be set to previously obtained optimal values from the optimization problem in Eq. (27), or may be set to the values obtained from a least-squares solution.

The second nonlinear programming approach for least-squares solution improvement is described next.

3.2 Parameter optimization: direct approach

A subset of system poles, as well as some additional coefficients to adjust the columns (rows) of the input (output) influence matrix, is used as optimization parameters. The optimizer adjusts these parameters to minimize the difference between the experimental transfer function and the identified transfer function over frequency range of interest. In this approach, the identified state matrix A is first transformed to a real Schur canonical form or modal form. The system poles, which reside on the diagonal elements or 2×2 block diagonal partitions of the state matrix, are directly changed via optimization. The additional design parameters include coefficients for a set of basis vectors, which affect the input (output) influence matrix. To minimize the number of optimization parameters, the smaller of the input or output influence matrices is chosen for parameterization. Assume that the input influence matrix is the smaller of the two, i.e., there are more outputs than inputs, and let (A, B_0, C, D) represent an initial realization for the identified system. Then, parameterize the input influence matrix B as

$$B = B_0 S + N_{B_0} R \tag{32}$$

where the matrix N_{B_0} is an $n \times q$ matrix whose column span the null space of the matrix B_0, that is

$$N_{B_0}^T B_0 = 0$$

14

and S and R are $r \times r$ and $q \times r$ coefficient matrices, respectively. An optimization problem, using an absolute error cost function, is discussed next using these parameters.

3.2.1 Absolute Error Cost Function: Direct Approach

The optimization problem is similar to the previous formulation derived for the eigenvalue assignment technique, and is summarized as

minimize J_3:

$$J_3 = ||G(z_k) - \widehat{G}(z_k)||_F \tag{33}$$

over

$$\text{blkdiag}(A), S, R$$

subject to

$$|\lambda(\text{blkdiag}(A)| < 1$$

Here, $\widehat{G}(z_k)$ represents the system realization given by

$$\widehat{G}(z_k) = C(z_k I_n - A)^{-1} B + D \tag{34}$$

The term blkdiag( ) denotes a subset of the 2×2 block diagonal of ( ). The constraint on the modulus of $\lambda(\text{blkdiag}(A))$ guarantees the stability of the identified system, and can be omitted if stability is not of concern. The number of poles (eigenvalues), that are used as design parameters, is specified the designer. One can use all the poles in the system, or just a few, for example, the real poles of the system. In real Schur form or modal form, the real poles (eigenvalues) are on the diagonal, while the pairs of complex conjugate poles (eigenvalues) reside in the 2×2 block diagonals, in the following form

$$\lambda_i = \begin{bmatrix} real(\lambda_i) & imag(\lambda_i) \\ -imag(\lambda_i) & real(\lambda_i) \end{bmatrix} \tag{35}$$

where the *real*( ) and *imag*( ) denote the real and imaginary parts, respectively. Care must be taken during parameterization to ensure those elements of the 2×2 block diagonals are parameterized properly so that complex conjugate pair remains intact throughout the optimization process.

15

In the next section, a complementary optimization problem is described using a relative error cost function.

3.2.2 Relative Error Cost Function: Direct Approach

A complementary optimization problem, wherein a norm of the relative error is optimized, may be used in order to provide a more equitable trade between errors in the peak and valley regions of the transfer function matrix. This optimization is defined as

$$J_4 = ||[G(z_k) - \widehat{G}(z_k)]./G(z_k)||_F \tag{36}$$

over

$$\text{blkdiag}(A), S, R$$

subject to

$$J_3 \leq J_{3_d}$$

$$|\lambda(\text{blkdiag}(A)| < 1$$

Here, J_3 is the Frobenius norm of the absolute error given by Eq. (33), J_{3_d} can be any desired value, but it is often set to a previously computed value for J_3 in Eq. (33), or the value of J from in initial least-squares solution. Similarly, the initial values of the design parameters may be set to the previously computed optimal values for the optimization problem of Eq. (33), or may be set to the values obtained from a least-squares solution.

The third nonlinear programming approach for least-squares solution improvement is described next.

3.3 Parameter optimization: Least-Squares

This method starts with selecting a subset of system poles as optimization parameters to minimize the error between the experimental and the identified transfer functions over frequency range of interest. The optimizer reassigns the system poles, which reside on the diagonal elements or 2x2 block diagonal partitions of the state matrix.

16

At each optimization step, corrections are made to the B, C, and D matrices through two least-squares solutions.

similar to the previous two nonlinear programming approaches, two optimization problems are presented in the next two sections, one using an absolute error cost function and the other using a relative error cost function.

3.3.1 Absolute Error Cost Function: Least-Squares

let (A, B_0, C_0, D_0) represent an initial realization for the identified system, and parameterize the input and output influence matrices as follows,

$$B = B_0 S_b + N_{B_0} R_B = \begin{bmatrix} B_0 & N_B \end{bmatrix} \begin{pmatrix} S_B \\ R_B \end{pmatrix} \equiv \overline{B} Q_B \qquad (37)$$

$$C = S_C C_0 + R_C N_{C_0} = \begin{pmatrix} S_C & R_C \end{pmatrix} \begin{bmatrix} C_0 \\ N_{C_0} \end{bmatrix} \equiv Q_C \overline{C} \qquad (38)$$

where the columns of N_{B_0} represent a set of basis vectors in the null space of B_0, the rows of N_{C_0} represent a set of basis vectors in the null space of C_0, and Q_B, defined in terms of S_B and R_B, and Q_C, defined in terms of S_C and R_C, are the appropriate coefficient matrices. These coefficients are determined, at each optimization step, by solving least-squares-based corrections of the absolute error norm. The optimization problem is given as

minimize J_5:

$$J_5 = ||G(z_k) - \widehat{G}(z_k)||_F \qquad (39)$$

over

$$\text{blkdiag}(A)$$

subject to

$$|\lambda(\text{blkdiag}(A))| < 1$$

The complex matrix $\widehat{G}(z_k)$ represents a system realization given by

$$\widehat{G}(z_k) = C(z_k I_n - A)^{-1} B + D \qquad (40)$$

The constraint on the modulus of $\lambda(\text{blkdiag}(A))$ guarantees the stability of the identified system, and can be omitted if stability is not of concern. At each optimization

17

step, as a new state matrix A is defined, corrections are performed to the B and D matrices via a least-squares solution, followed by corrections to the C and D matrices. These solutions are defined next.

First, let $\overline{G}(z_k) = G(z_k) - D$, and repartition the $n_d \times (m \times r)$ transfer function matrix, $\overline{G}(z_k)$, columnwise, such that each column of the repartitioned $(n_d \times m) \times r$ matrix, $\overline{G}_{col}$, is associated with an input.

Define $\widehat{\overline{G}}(z_k) = C_0(z_k I_n - A)^{-1}\overline{B}$, repartition $\widehat{\overline{G}}(z_k)$ similar to $\overline{G}_{col}$ to obtain $\widehat{\overline{G}}_{col}$, and define the absolute error function as

$$e = \overline{G}_{col} - \widehat{\overline{G}}_{col}Q_B \tag{41}$$

Now, solve for Q_B, in a least-squares sense, to obtain

$$Q_B = (\widehat{\overline{G}}_{col}^T \widehat{\overline{G}}_{col})^{-1}\widehat{\overline{G}}_{col}^T \overline{G}_{col} \tag{42}$$

Once, Q_B is computed, then D is computed as

$$D = \mu\left(G(z_k) - C_0(z_k I_n - A)^{-1}B\right) \tag{43}$$

where $\mu(\ )$ denotes the mean over frequency points.

To compute Q_C, first define $\overline{G}(z_k) = G(z_k) - D$, and repartition the $n_d \times (m \times r)$ transfer function matrix, $\overline{G}(z_k)$, rowwise, such that each row of the repartitioned $m \times (n_d \times r)$ matrix, $\overline{G}_{row}$, is associated with an output. Define $\widehat{\overline{G}}(z_k) = \overline{C}(z_k I_n - A)^{-1}B$, repartition $\widehat{\overline{G}}(z_k)$ similar to $\overline{G}_{row}$ to obtain $\widehat{\overline{G}}_{row}$, and define the error function as

$$e = \overline{G}_{row} - Q_C\widehat{\overline{G}}_{row} \tag{44}$$

Now, solve for Q_C, in a least-squares sense, to obtain

$$Q_C = \overline{G}_{row}\widehat{\overline{G}}_{row}^T(\widehat{\overline{G}}_{row}\widehat{\overline{G}}_{row}^T)^{-1} \tag{45}$$

Once, Q_C is computed, then D is recomputed as

$$D = \mu\left(G(z_k) - C(z_k I_n - A)^{-1}B\right) \tag{46}$$

The number of poles (eigenvalues) that can be used as design parameters is somewhat arbitrary. One may use all the poles in the system, or just a few, for example, the real poles of the system.

3.3.2 Relative Error Cost Function: Least-Squares

Similar to the previous cases, the cost function is written in terms of a norm of the relative error to provide a more equitable trade between errors in the peak and valley regions of the transfer function matrix. This optimization problem is defined as: *minimize J_6:*

$$J_6 = ||[G(z_k) - \widehat{G}(z_k)]./G(z_k)||_F \qquad (47)$$

over

$$\text{blkdiag}(A)$$

subject to

$$J_5 \leq J_{5_d}$$

$$|\lambda(\text{blkdiag}(A)| < 1$$

Here, J_5 is the Frobenius norm of the absolute error given by Eq. (39), J_{5_d} can be any desired value, but it is often set to a previously computed value for J_5 in Eq. (39), or the value of J from in initial least-squares solution. Similarly, the initial values of the design parameters may be set to the previously computed optimal values for the optimization problem of Eq. (39), or may be set to t he values obtained from a least-squares solution. The transfer function matrix $\widehat{G}(z_k)$ is the same as that used for the pervious optimization problem, and is provided by Eq. (40), and the input and output influence matrices B and C are expanded following Eqs. (37)-(38).

Now, there are two possible approaches for performing the least-squares-based corrections to the B, C, and D matrices. The first approach is to use the procedure outlined earlier for computing the coefficient matrices Q_B (Eq. (42)) and Q_C (Eq. (45)), exactly. That procedure is based on a least-squares correction of the absolute error norm. The second approach is to compute these coefficient matrices from a least-squares correction of the relative error norm. However, the least-squares problems, whose solutions yield the coefficient vectors Q_B and Q_C, are somewhat different because they use a relative error norm instead of an absolute error norm. Without going into details of this alternative, the equations are fairly similar to those obtained for the absolute error case, with three exceptions. First, instead of two least-squares

19

problems, one for input influence matrix correction and one for output influence matrix correction, there would be r least-squares problems for the input influence matrix correction, one for each column of the B matrix, and m least-squares problems for the output influence matrix correction, one for each row of the C matrix. The second exception is that one column (row) of the matrix $\overline{G}_{col}$ ($\overline{G}_{row}$), at a time, is used for each least-squares problem, with all its elements replaced by ones. The last exception is that the columns (rows) of $\overline{G}_{col}(\overline{G}_{row})$ are normalized by the elements of $\overline{G}_{col}(\overline{G}_{row})$.

4 Applications

This section describes the application of the proposed techniques to the system identification for the PARTI wind-tunnel model [12], a laboratory test structure at NASA Langley. The model is a five-foot long, high aspect ratio wing designed to flutter at low speeds to simplify aerodynamic analyses and wind-tunnel testing. The fully assembled semi-span model is shown in Fig. 1. The model has a total of 72 actuators bonded to both sides of the plate. Each actuator contains two stacks of two 0.01 inch piezoelectric patches. The 72 actuators are hardwired to actuate in 15 different groups. The 15 groupings were chosen such that each group primarily affects one of the first three natural modes. Each group can be considered as one input, because all the actuators in the group use the same signal. The piezoelectric patches were only used for actuation; ten strain gages and four accelerometers were used as sensors. As a result, there are a total of 15 inputs and 14 outputs.

4.1 Weighted Least-Squares Solution

In the first application, the transfer function from input No. 1 to all outputs is considered for identification. With signals from 14 sensor outputs ($m = 14$), input No. 1 ($r = 1$), and 10th order polynomials ($p = 10$) used in the matrix-fraction expansion (see Eqs. (1)-(3)), a weighted least-squares solution was first obtained from Eq. (22), using an exponential weighting function, given as

$$w^k \; ; \quad k = 0, 1, \ldots, \ell$$

Here, $k = 0$ refers to the zero frequency component of the FRF often known as the direct current (DC) term in electrical engineering, and w was chosen at 0.98. By adjusting the value of w one may emphasize the low frequencies or the higher frequencies. Values of w less than 1 would emphasize the lower end of the frequency spectrum. Here, w was set to 0.98, to emphasize the range of frequency from 0 to 25 Hz. The weighted least-squares solution resulted in an identified model of order 140, which included 4 unstable poles. However, since the actual testbed is stable, it is desired to obtain a stable identified model. Truncating the unstable states yielded a 136-order state-space realization of the system. Magnitude and phase FRF plots for outputs No. 7 and 10 are shown in Figs. 2 and 3, respectively.

Comparison of the plots indicates an excellent agreement between the experimental FRF (solid line) and the identified FRF (dashed line), particularly around the peaks of the FRF or where the gain values are significant. However, discrepancies can be observed around some of the zeros as well as where the gain values are small. This should be expected as the least-squares problem is dominated by the peaks and large gain values. Further inspection of these plots also indicates that the agreement between the experimental and identified results is better in the 0-25 Hz range. The Frobenius norm of the error between the experimental and identified transfer functions was computed at 90.128, the majority of which is due to the differences between two FRFs at DC frequency. In fact, since the DC gain values are quite large, particularly in some output channels, they tend to dominate the rest of the FRF in a least-squares solution. Keep in mind that the DC gain values may not be accurate due to the use of accelerometers and their insensitivity at very low frequencies, drift problems that hampers accurate measurements, and lack of sufficient data. Therefore, in this case, it is reasonable to de-emphasize the DC values by assigning a zero value to the corresponding weighting function, such that the DC weight is set to zero. The Bode plots, using the *modified weighting function*, are shown in Figs. 2 and 3 as dashed-dotted lines. These figures indicate moderate improvements in various frequency ranges. The Frobenius norm of the error between the experimental and identified transfer functions was computed at 90.134, a very minor change from the

21

previous results, indicating that little in terms of minimizing the overall error is lost. Comparing, the norm of the error for all frequency points except DC, shows that the error went down from 0.241 to 0.223, which quantifies the better match by using the modified weighting function.

In order to show the effectiveness of the modified exponential weighting, a polynomial with $p = 3$ is used in the matrix-fraction description. The weighted least-squares solution resulted in a stable identified model of order 40. Figures 4 and 5 illustrate the stable least-squares solutions for the nominal and modified exponential weightings for outputs No. 7 and 10. These figures clearly demonstrate the advantage of modified exponential weighting for this problem. In fact, the Frobenius norm of the error between the experimental and identified transfer functions dropped from 12.035 to 0.3021, a significant improvement.

4.2 Further Enhancements: Nonlinear Programming

To demonstrate the potential of the nonlinear programming approaches to further enhance the least-squares solution, the direct optimization approach is applied to an identified model for the PARTI testbed, obtained from a least-squares solution. Three optimization problems were considered and carried out in this application. The first optimization approach was the one posed in Eq. (33), minimizing the Frobenius norm of the absolute error cost function for all frequency points except the DC, using as design variables the real poles of the identified plant as well as the coefficients of the basis vectors, S and R, from Eq. (32). The initial least-squares solution provided a stable model of order 40, with 6 real poles. This model was transformed into modal form to make it amenable to optimization with the direct approach. There were 26 design variables used in the optimization, the first 6 being the values of the real poles of the system, the 7th representing the coefficient S (see Eq. (32)), and the remaining 19 representing the elements of the coefficient vector R (see Eq. (32)), corresponding to 19 basis vectors from the null space of the matrix B_0. It should be noted that one could have included the complex poles of the system as design variables too. However, it was concluded that this may not be necessary since the dominant poles (resonances)

22

of the system were captured by the least-squares solution, as observed from Figs. 4 and 5. The optimization included 7 constraints, the first six to assure the stability of the system as the poles were reassigned, and the last constraint on the value of the error norm to avoid convergence to undesirable local minima. The optimization was performed using the Automated Design Synthesis (ADS) software [13]. The interior penalty function method of ADS was used to solve the nonlinear programming problems. In this method, the constrained optimization problem is transformed into an unconstrained problem through creation of a objective function which is the sum of the original objective function and an imposed penalty function (which is a function of the constraints) [14]. The initial solution used in the optimization was that of stable least-squares solution with modified exponential weighting. The optimization reduced the norm of the absolute error from the initial value of 0.302 to 0.285. The optimization was repeated once with a new input influence matrix bases. These bases included the initial influence vector, along with a new set of 19 random basis vectors from the null space of the matrix $[B_0 \quad N_{B_0}]$. The second optimization run reduced the norm of the error from 0.289 to 0.249, which is fairly close to 0.223, the error norm corresponding to the stable least-squares solution with $p = 10$. This process could have been continued further, however, it was deemed that the computational burden would outweigh any additional reductions in the norm of the error. The Bode plots, comparing the transfer function matrices for the experimental, nominal, and optimal results are provided in Figs. 6 and 7, for output No. 7 and 10, where it is observed that the identified model, via optimization, performs well, almost at a comparable level to that for $p = 10$. This is very encouraging, considering that the optimization-based model is a 40th order model compared to 136th order model for $p = 10$.

Figures 6 and 7 also indicate that there is room for improving the test and analysis agreement around the transmission zeros and low gain regions. To accomplish this, a second optimization problem was performed. This case used the formulation described in Eq. (36), in which the Frobenius norm of the relative error is minimized. The initial design used the optimal solution obtained from the first optimization problem. Similar

23

to the first optimization, 26 design variables were used in the optimization, the first 6 being the location of the real poles of the system; the 7th represents the coefficient S (see Eq. (32)); and the remaining 19 representing the elements of the coefficient vector R (see Eq. (32)), corresponding to 19 basis vectors from the null space of the matrix B_0. In addition, 7 constraints were used, the first six to guarantee system stability, and the last constraint to ensure that the Frobenius norm of the absolute error remained equal to or below 0.249, the level obtained by the first optimization. The optimization reduced the norm of the relative error from the initial value of 181.11 to 152.48. The optimization was repeated once more with a set of new input influence matrix bases. The second optimization run reduced the norm of the error from 152.48 to 118.34, and the optimization process was terminated. The Bode plots for the experimental, nominal, and optimal results, for outputs No. 7 and 10, are presented in Figs. 8 and 9. These figures illustrates a considerable improvement in the optimal model in matching the area around the transmission zeros and low gain regions of the transfer functions. These results demonstrate the advantages of further enhancements to the least-squares solution.

Another optimization problem considered was the problem posed in Eq. (39) where the Frobenius norm of the absolute error is minimized while adjusting the eigenvalues of the state matrix, subject to stability constraints. Moreover, the optimization included corrections to the B and D matrices, followed by corrections to the C and D matrices, at each functional evaluation (see Eq. (42)-(43) and (45)-(46)). The 6 design variables used in the optimization were the values of the real poles of the system. The optimization included 7 constraints, the first six to guarantee the stability of the systems as the poles were reassigned, and a constraint on the value of the error norm to avoid undesirable local minima. The initial design used in the optimization was was taken from a stable least-squares solution with modified exponential weighting, i.e., zero DC weighting. The optimization reduced the norm of the absolute error from the initial value of 0.250 to 0.197, which is over 20% reduction. Plots, comparing the transfer function matrices for the experimental, nominal, and optimal results are provided in Figs. 10 and 11, for output No. 7 and 11. The identified model (via

24

optimization) agrees very well with the experimental data. Also note that output 11 is now shown as opposed to 10 in the previous cases. This output sensor shows modes around 28 and 38 Hz which are also being identified.

All the identification results obtained so far were based on the 14 transfer functions from the first input to all 14 outputs. Now, let us consider the transfer functions from all 15 inputs to all 14 outputs for identification. With the signals from all 14 sensor outputs ($m = 14$) and all 15 inputs ($r = 15$), and 3rd order polynomials ($p = 3$) used in the matrix-fraction expansion(see Eqs. (1)-(3)), a weighted least square solution was first obtained from Eq. (22). Similar to the previous cases, an exponential weighting function was used, with parameter w chosen at 0.98 to emphasize the range of low frequencies. In addition, the DC weight was set to zero. The Frobenius norm of the error between the experimental and identified transfer functions was computed at 246.855, the majority of which is due to a discrepancy between two FRFs at the DC frequency, i.e., zero frequency. The Frobenius norm of the absolute error, for all frequency points except the DC, was computed to be 1.721. For the purpose of illustration, plots for the experimental and realized transfer functions are depicted in Figs. 12 and 13, for outputs No. 7 and 11 with input No. 1, and in Figs. 14 and 15, for the same outputs with input No. 8. The experimental transfer functions are shown as solid lines and the transfer functions, obtained via direct least square, as dashed lines. These figures indicate moderate to good agreement between the transfer functions in low frequencies ranges, particularly, around the peaks or high gain areas of the transfer functions.

Now consider the least-squares optimization approach presented in Eq. (39) for the 15 inputs and 14 output case. The initial design used in the optimization was the stable least-squares solution with modified exponential weighting. This realization had 14 real poles, whose locations were used as design variables in the optimization, i.e., there were 14 design variables. The optimization included 15 constraints, the first 14 to guarantee the stability of the systems as the poles were reassigned, and the last constraint on the value of the error norm to avoid convergence to undesirable local minima. The optimization reduced the norm of the error from the initial value of

1.165 to 1.090, about a 6.5% reduction. Plots, comparing for the experimental (solid line), nominal (dashed line), and optimal transfer function (dashed-dotted line) are provided in Figs. 12 through 15. It is observed that the identified model (obtained via optimization) performs well, although only 3rd order polynomials was used in the matrix fraction description to match a 15 input by 14 output transfer function. Comparison of Figs. 12 and 13 with Figs. 10 and 11, which correspond to the same input and output channels, and were obtained from a single input identification problem, reconfirms the good level of correlation obtained following the optimization-based approach.

5 Concluding Remarks

Several techniques have been presented to identify an experimental system model directly from frequency response data. The techniques used a matrix-fraction description (MFD) to describe the identified system. The MFD coefficients were obtained from the solution of a weighted least-squares problem. Frequency weighting concepts were introduced in order to emphasize a frequency range of interest. Three optimization-based methods were introduced to fine-tune the experimentally realized models. The first method uses an eigenvalue assignment technique to reassign a subset of the system poles to enhance the approximation of the identified model. The second method considers the model in the real Schur or modal form, and uses a subset of system poles as well as additional parameters to adjust the columns (rows) of the input (output) influence matrix in order to improve the model fit. The third method optimizes a subset of the system poles, while the input and output influence matrices are computed at every optimization step through least-squares procedure. The methods were applied to data from PARTI wind tunnel model, a laboratory testbed at NASA Langley Research Center. The benefits of the optimization-based refinement techniques as well as frequency weighting techniques were demonstrated. It was shown that with optimal fine-tuning and proper choice of frequency weighting a 40th order system realization could provide almost the same level of model fit as a full-order

26

136th order model. Specifically, the third optimization method provided the largest improvement in the fit of the experimental data, with a 20-percent smaller absolute error norm than that obtained from the second optimization method. However, the computational cost of performing the third optimization formulation was considerably higher than the second optimization problem, primarily due to the large least-squares solutions that were solved at every optimization step to perform corrections to the B, C, and D matrices. The optimizations used finite difference techniques to provide gradient information on the objective function and constraints. The numerical computation of the gradients may require a large number of functional evaluation, which would be costly in a computational sense. Alternatively, one may attempt to obtain analytical expressions for the gradients, and perhaps second-order partial derivatives, to improve computational efficiency and accuracy.

References

[1] Juang, J.-N. and Suzuki, H., "An Eigensystem Realization in Frequency Domain for Modal Parameter Identification," *Journal of Vibration, Acoustics, Stress and Reliability in Design,* Vol. 110, No. 1, January 1988, pp. 24-29.

[2] Bayard, D. S., "An Algorithm for State Space Frequency Domain Identification without Windowing Distortions," *Proceedings of the Control and Decision Conference,* December 1992.

[3] Chen, C. W., Juang, J.-N., and Lee, G., "Frequency Domain State-Space System Identification," *Transactions of the ASME, Journal of Vibration and Acoustics,* Vol. 116, No. 4, Oct. 1994, pp. 523-528

[4] Horta, L. G., Juang, J.-N., and Chen, C.-W., "Frequency Domain Identification Toolbox," *NASA Technical Memorandum 109039,* September 1996, pp. 1-28.

[5] Juang, J.-N., *Applied System Identification,* Prentice Hall, Inc., Englewood Cliffs, New Jersey 07632, 1994, ISBN 0-13-079211-X.

[6] Chen, C.-W., Juang, J.-N., and Lee, G., "Stable State Space System Identification from Frequency Domain Data," *Proceedings of the first IEEE Regional Conference on Aerospace Control Systems*, CA., May 25-27, 1993.

[7] Astrom, K.J., and Witenmark, B., *Adaptive Control*, Addison-Wesley Publishing Company, 1995.

[8] Gill, P. E., Murray, W., and Wright, M. H., *Practical Optimization*, John Academic Press, London, 1981.

[9] Juang, J. N., Lim, K. B., and Junkins, J. L., "Robust Eigensystem Assignment for Flexible Structures," *Journal of Guidance, Control and Dynamics*, Vol. 12, No. 3, May-June 1989, pp. 381-387.

[10] Maghami, P. G., and Juang, J. N., "Efficient Eigenvalue Assignment for Large Space Structures," *Journal of Guidance, Control and Dynamics*, Vol. 13, No. 6, Nov.-Dec. 1990, pp. 1033-1039.

[11] Juang, J. N., and Maghami, P. G., "Robust Eigensystem Assignment for Second Order Dynamics System," *Mechanics and Control of Large Space Structures* edited by John L. Junkins, AIAA Monograph on Progress in Astronautics and Aeronautics, Vol 29, 1990, pp. 373-387.

[12] McGowan, A. R., Heeg, J., and Lake, R. C., "Results of Wind-Tunnel Testing from the Piezoelectric Aeroelastic Response Tailoring Investigation," 1996 Structures, Structural Dynamics, and Materials Conference.

[13] Vanderplaats, G. N., "ADS - A FORTRAN Program for Automated Design Synthesis - Version 1.1," NASA CR-177985, 1985.

[14] Vanderplaats, G. N., "Numerical Optimization Techniques for Engineering Design - with Applications," McGraw-Hill, Inc., 1984.
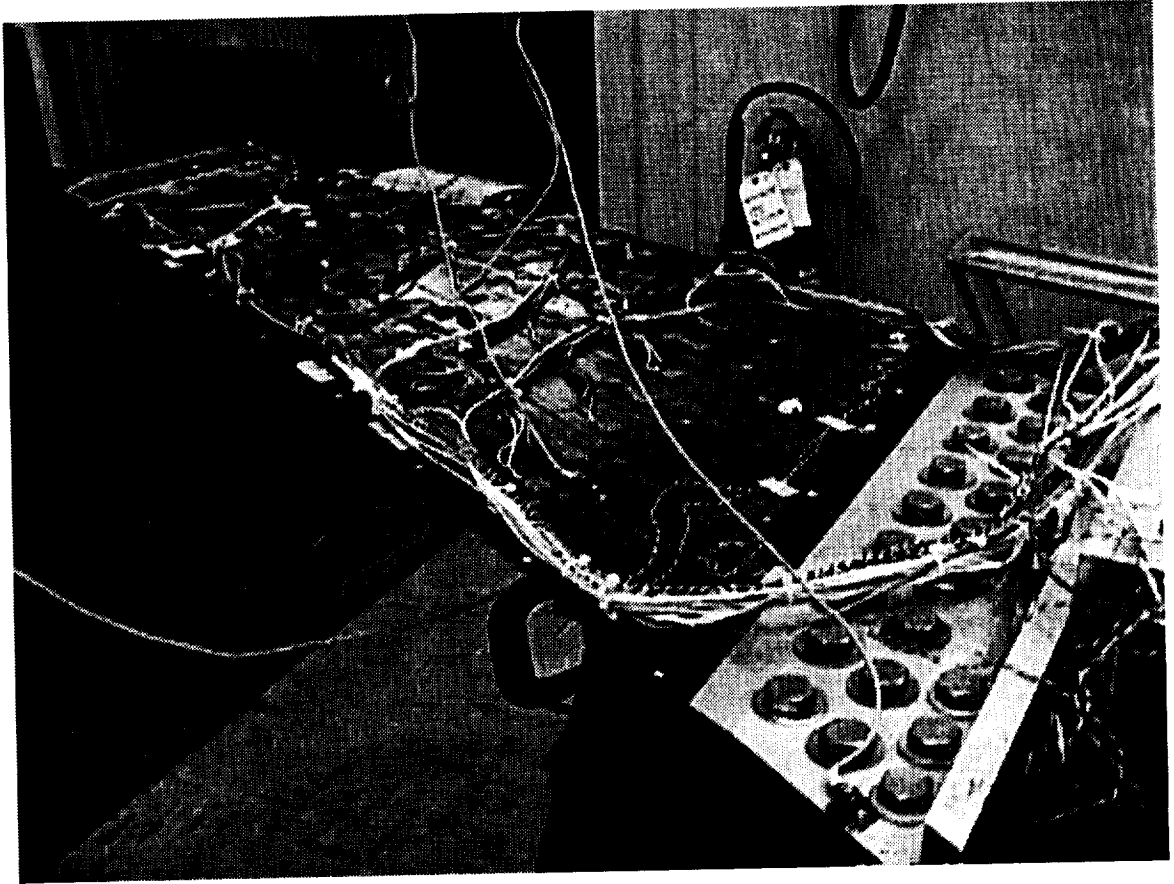
Figure 1: PARTI Model
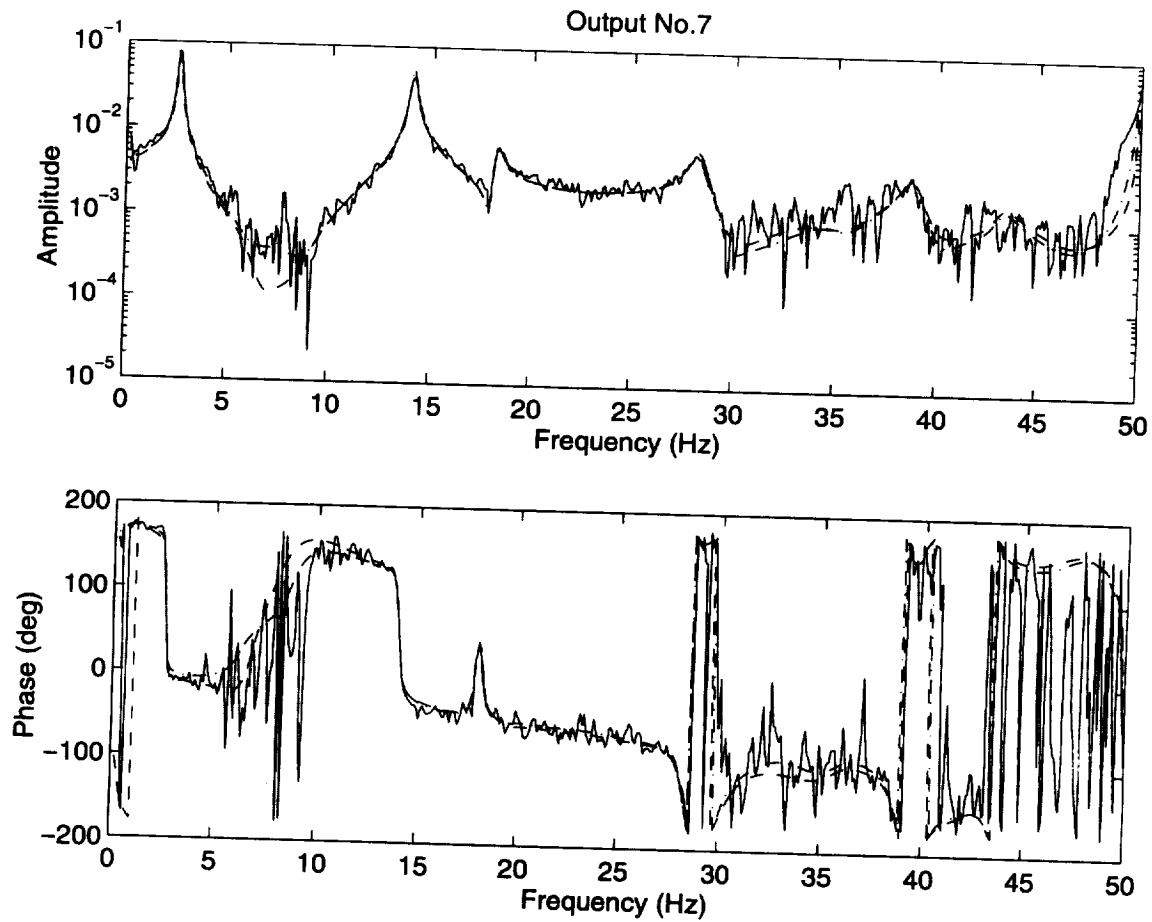
Figure 2: Comparison of FRFs for Output No. 7 with exponential weighting and 136-order system: experimental FRF (solid line), identified FRF (dashed line), identified FRF with zero DC weighting (dashed-dotted line).
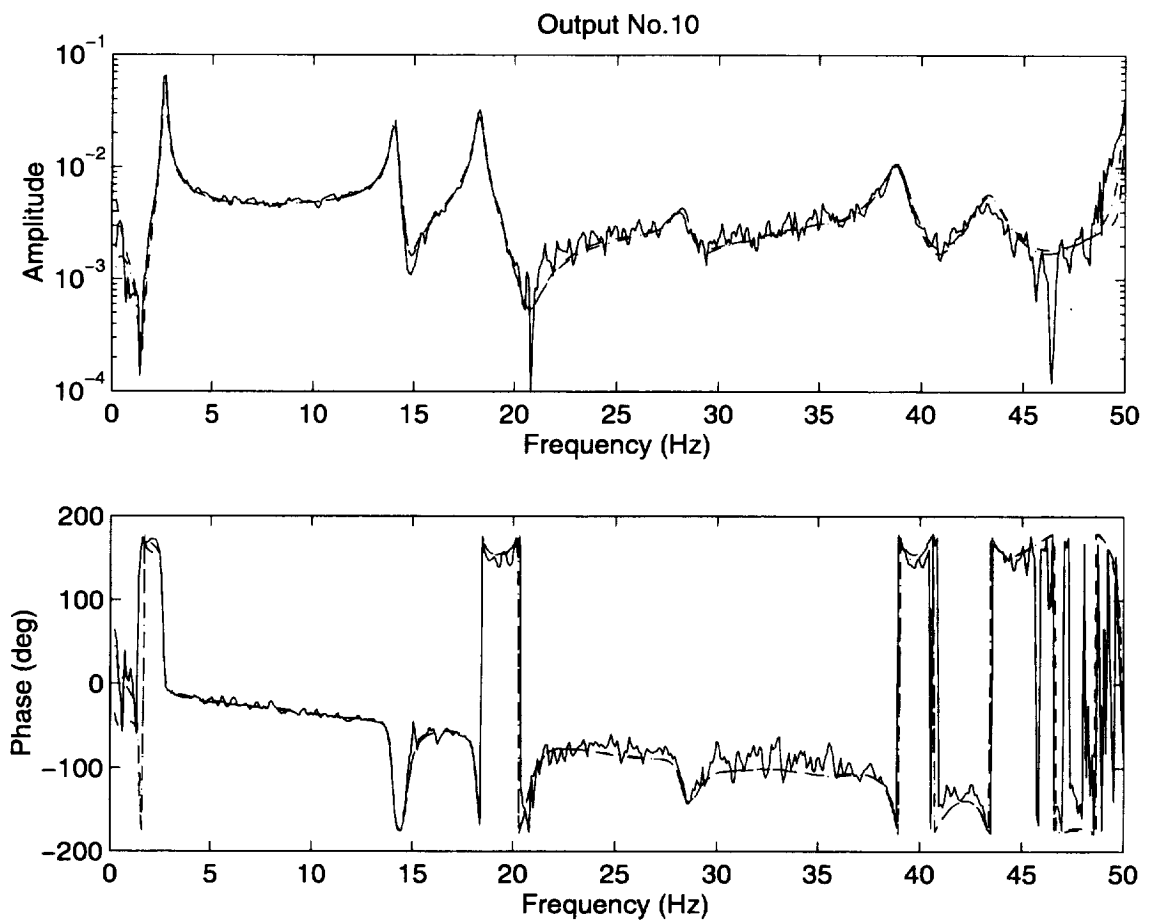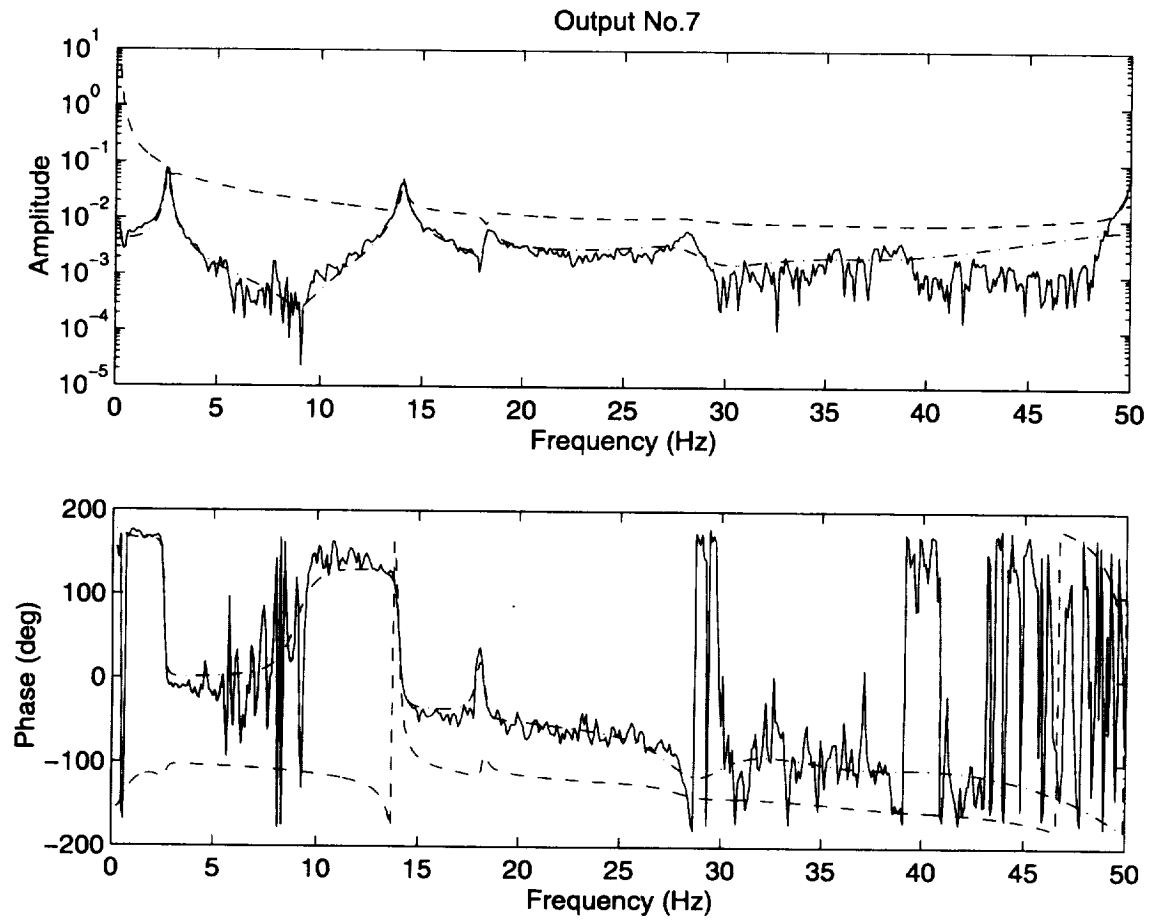
Figure 3: FRF for Output No. 10 with exponential weighting and 136-order system: experimental FRF (solid line), identified FRF (dashed line), identified FRF with zero DC weighting (dashed-dotted line)
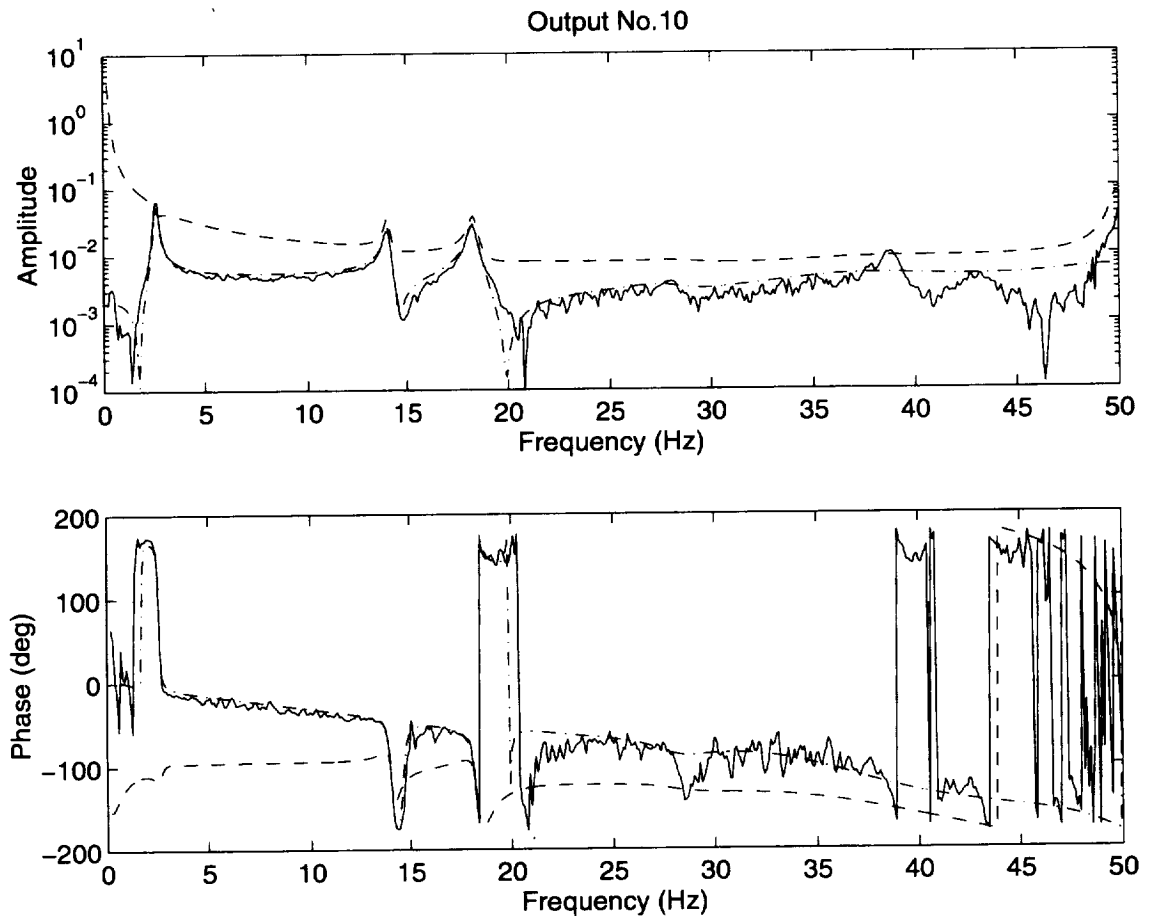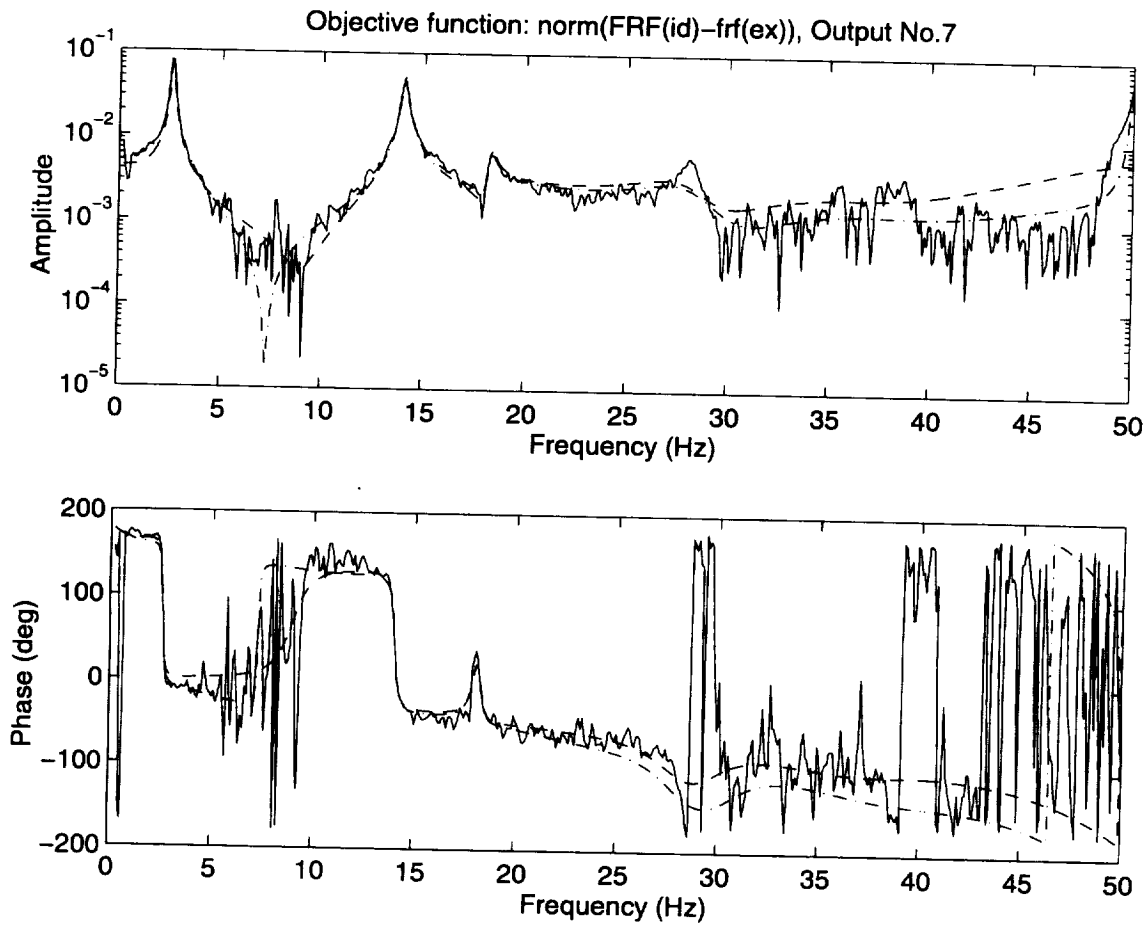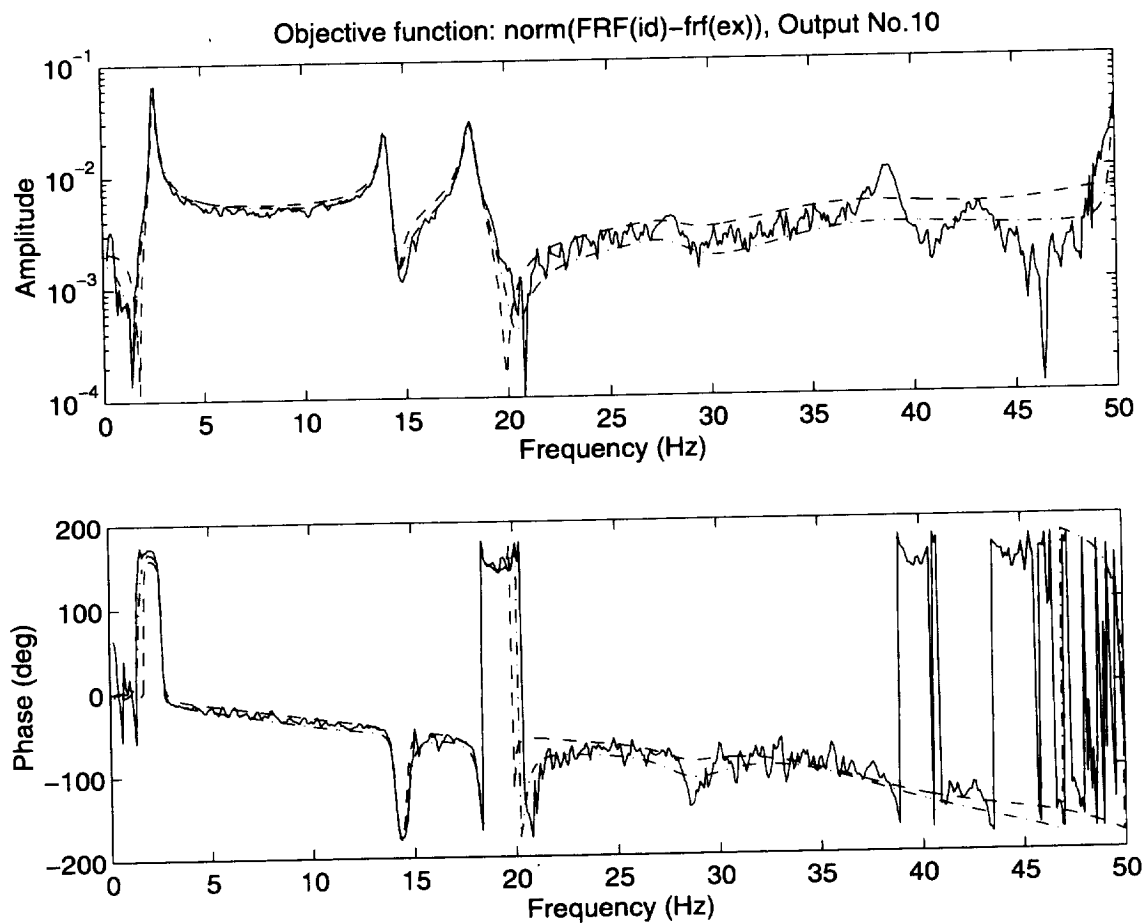
31

Figure 4: Comparison of FRFs for Output No. 7 with exponential weighting and 40-order of system: experimental FRF (solid line), identified FRF (dashed line), identified FRF with zero DC weighting (dashed-dotted line)

Figure 5: Comparison of FRFs for Output No. 10 with exponential weighting and 40-order of system: experimental FRF (solid line), identified FRF (dashed line), identified FRF with zero DC weighting (dashed-dotted line)
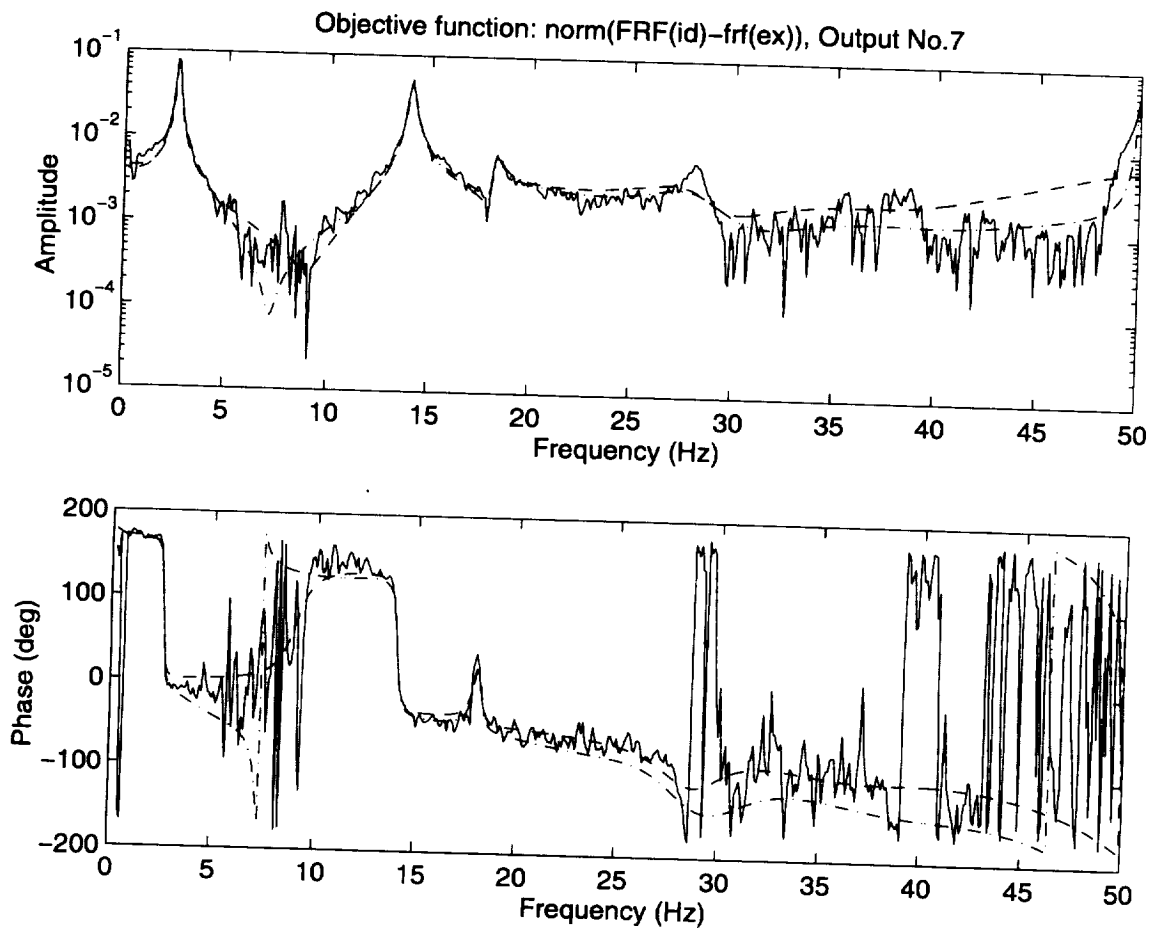
33

Figure 6: Comparison of FRFs for Output No. 7 with direct optimization approach and 40-order system: experimental FRF (solid line), identified FRF (dashed line) with zero DC weighting, enhanced FRF with absolute-error optimization (dashed-dotted line)
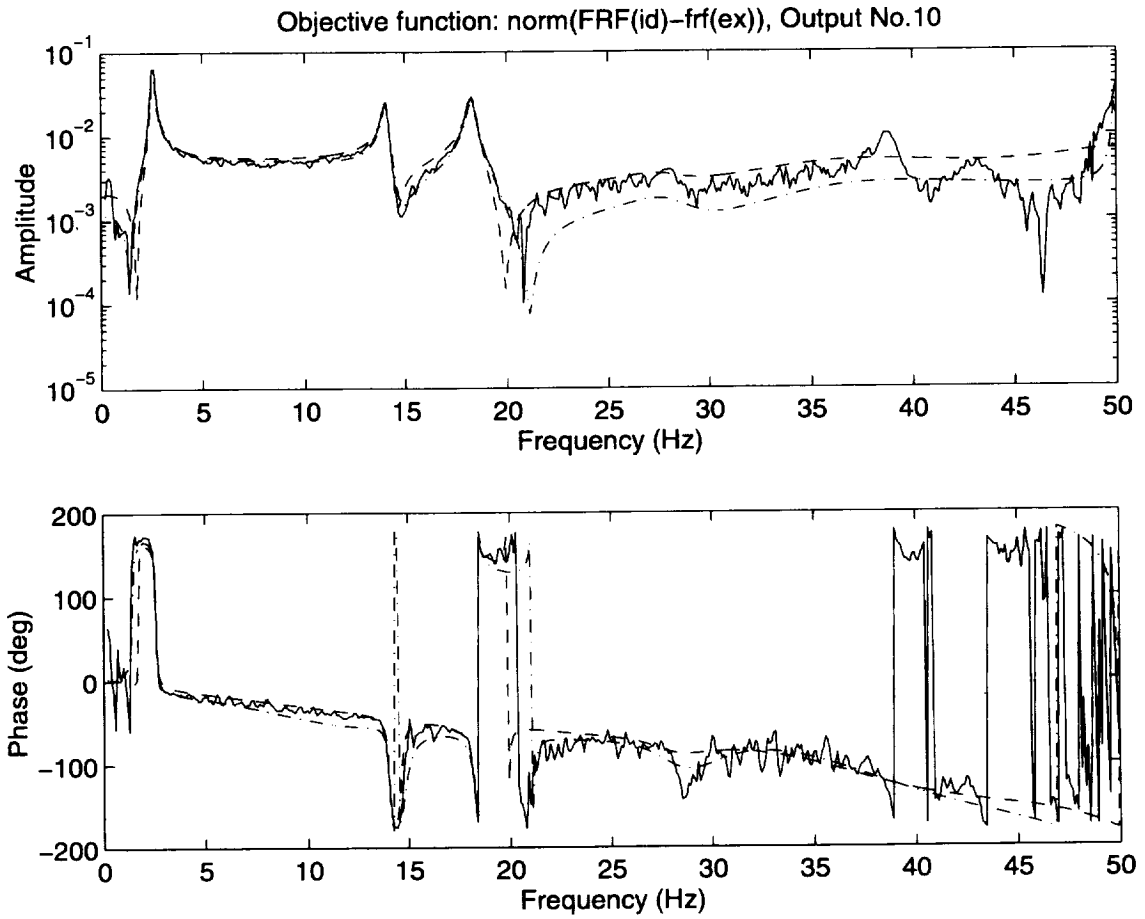
Figure 7: Comparison of FRFs for Output No. 10 with direct optimization approach and 40-order system: experimental FRF (solid line), identified FRF (dashed line) with zero DC weighting, enhanced FRF with absolute-error optimization (dashed-dotted line)

Figure 8: Comparison of FRFs for Output No. 7 with direct optimization approach and 40-order system: experimental FRF (solid line), identified FRF (dashed line) with zero DC weighting, enhanced FRF with relative-error optimization (dashed-dotted line)

36

Figure 9: Comparison of FRFs for Output No. 10 with direct optimization approach and 40-order system: experimental FRF (solid line), identified FRF (dashed line) with zero DC weighting, enhanced FRF with relative-error optimization (dashed-dotted line)
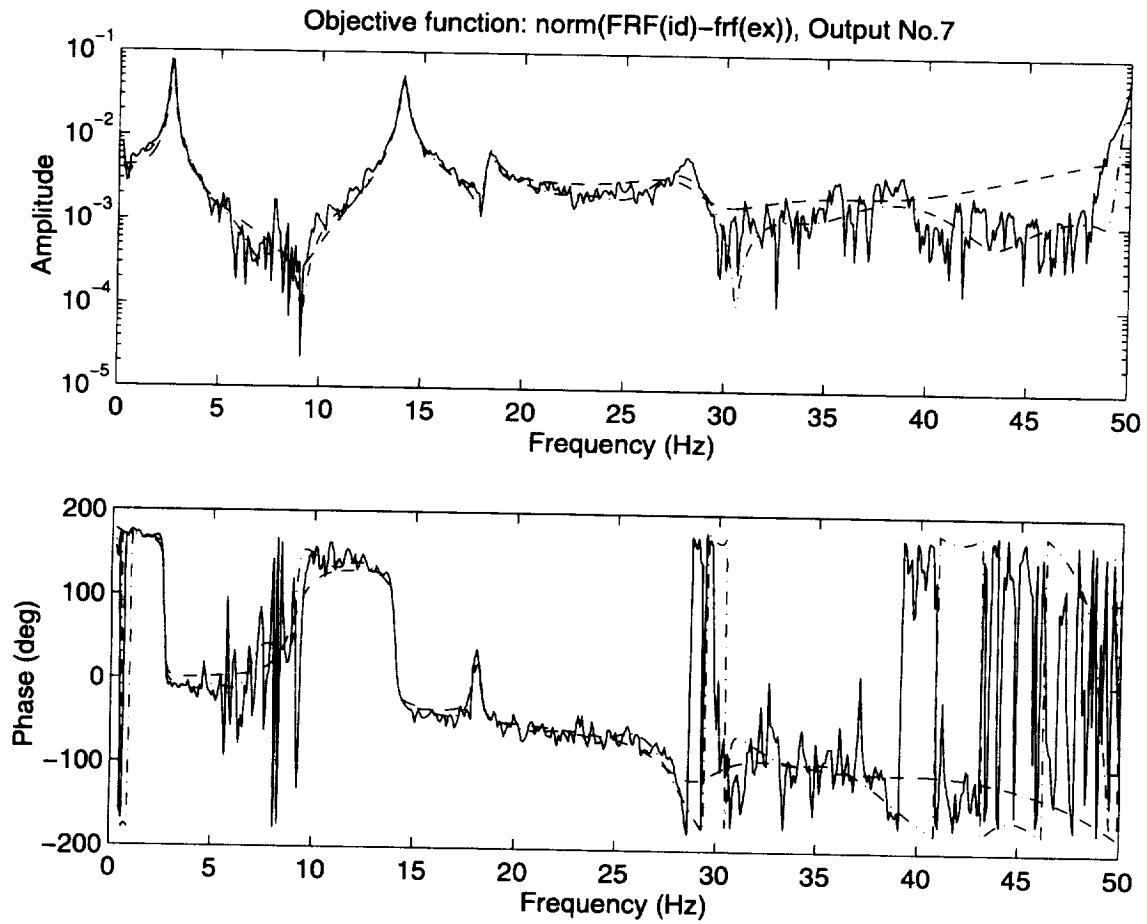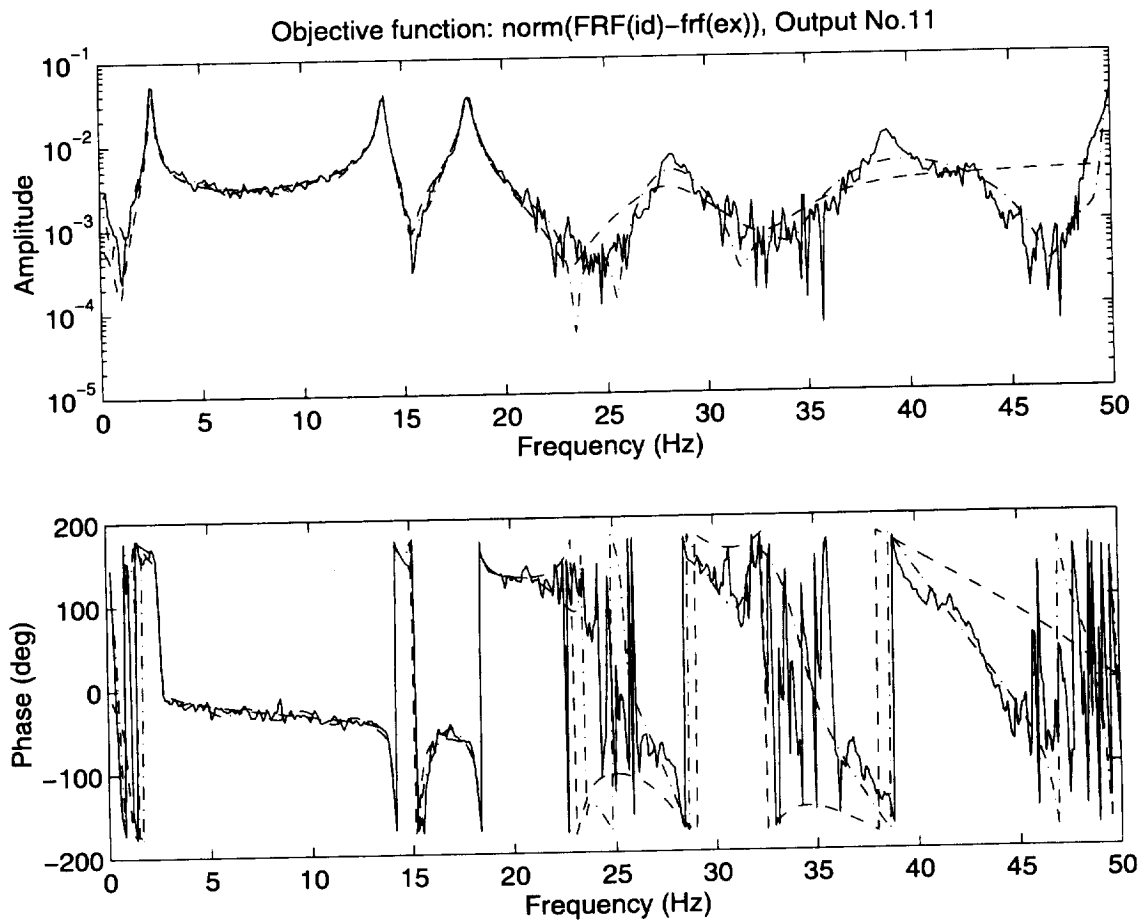
Figure 10: Comparison of FRFs for Output No. 7 with least-squares optimization approach and 40-order system: experimental FRF (solid line), identified FRF (dashed line) with zero DC weighting, enhanced FRF with absolute-error optimization (dashed-dotted line)

Figure 11: Comparison of FRFs for Output No. 11 with least-squares optimization approach and 40-order system: experimental FRF (solid line), identified FRF (dashed line) with zero DC weighting, enhanced FRF with absolute-error optimization (dashed-dotted line)
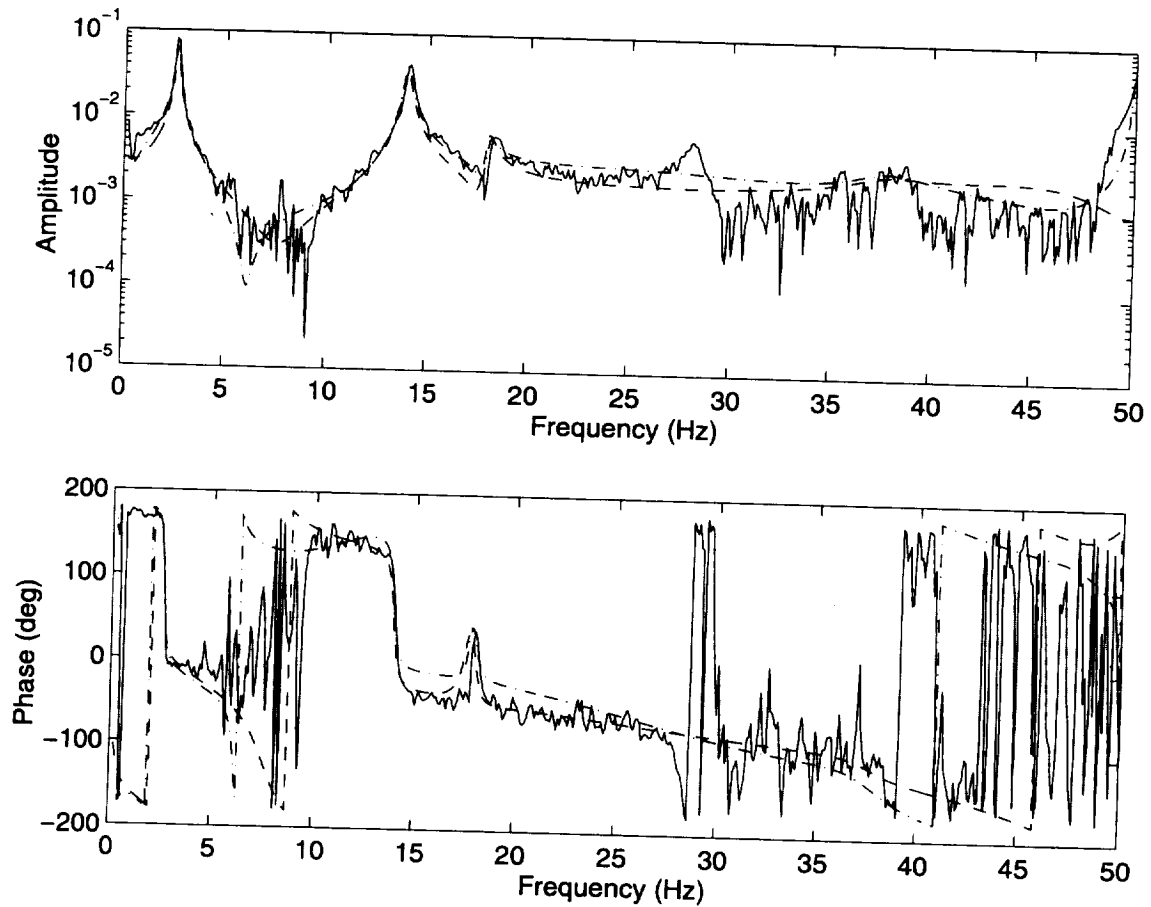
Figure 12: Comparison of FRFs for Output No. 7 and Input No. 1 with least-squares optimization approach and 42-order system: experimental FRF (solid line), identified FRF (dashed line) with zero DC weighting, enhanced FRF with absolute-error optimization (dashed-dotted line)
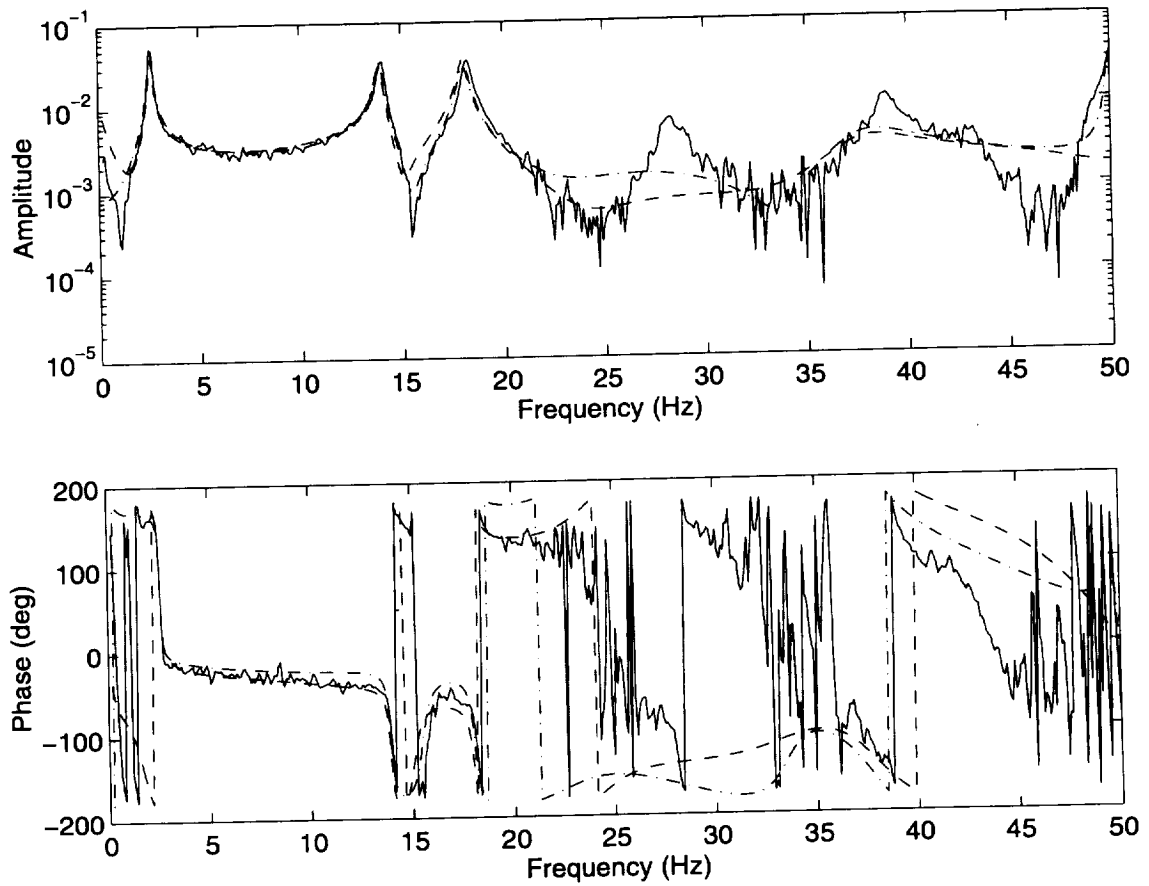
40

Figure 13: Comparison of FRFs for Output No. 11 and Input No. 1 with least-squares optimization approach and 42-order system: experimental FRF (solid line), identified FRF (dashed line) with zero DC weighting, enhanced FRF with absolute-error optimization (dashed-dotted line)
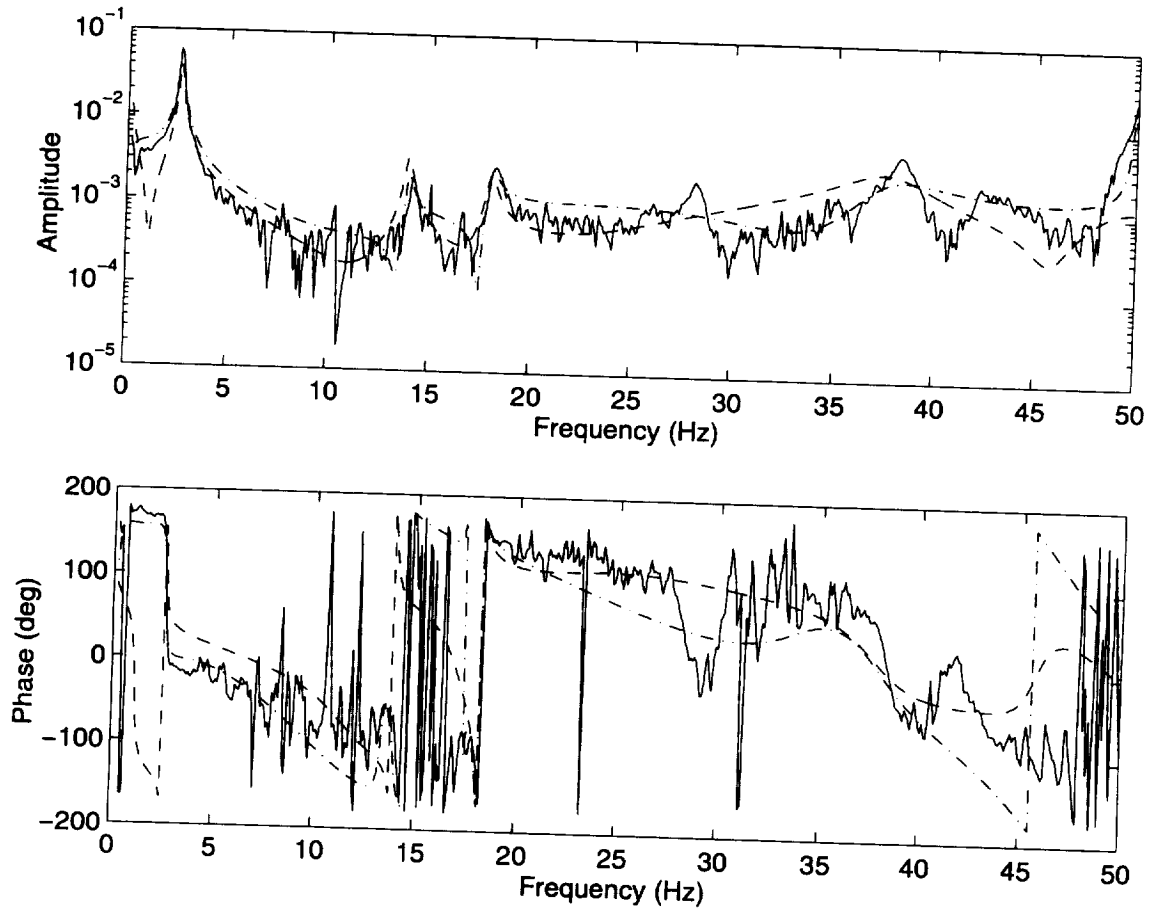
41

Figure 14: Comparison of FRFs for Output No. 7 and Input No. 8 with least-squares optimization approach and 42-order system: experimental FRF (solid line), identified FRF (dashed line) with zero DC weighting, enhanced FRF with absolute-error optimization (dashed-dotted line)
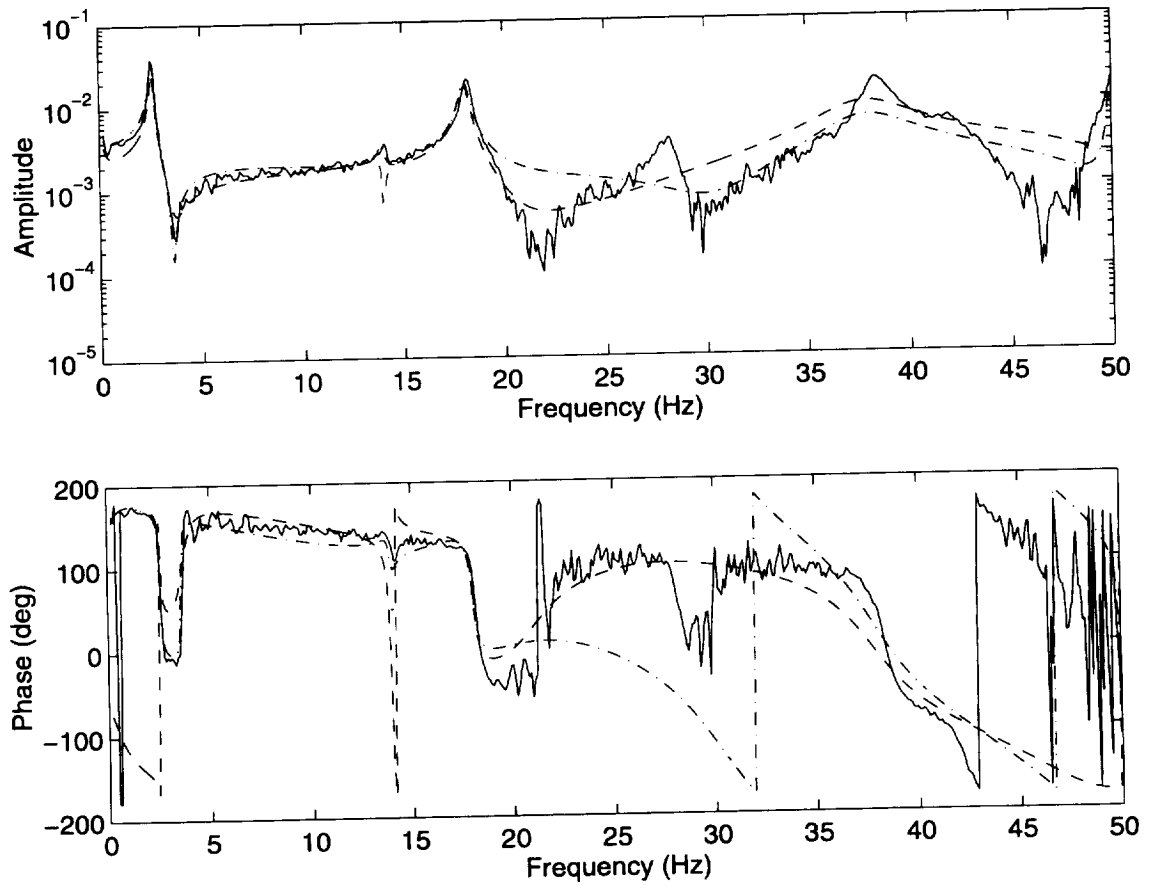
Figure 15: Comparison of FRFs for Output No. 11 and Input No. 8 with least-squares optimization approach and 42-order system: experimental FRF (solid line), identified FRF (dashed line) with zero DC weighting, enhanced FRF with absolute-error optimization (dashed-dotted line)

REPORT DOCUMENTATION PAGE

Form Approved
OMB No. 0704–0188

Public reporting burden for this collection of information is estimated to average 1 hour per response, including the time for reviewing instructions, searching existing data sources, gathering and maintaining the data needed, and completing and reviewing the collection of information. Send comments regarding this burden estimate or any other aspect of this collection of information, including suggestions for reducing this burden, to Washington Headquarters Services, Directorate for Information Operations and Reports, 1215 Jefferson Davis Highway, Suite 1204, Arlington, VA 22202–4302, and to the Office of Management and Budget, Paperwork Reduction Project (0704–0188), Washington, DC 20503.

1. AGENCY USE ONLY *(Leave blank)*	2. REPORT DATE April 1999	3. REPORT TYPE AND DATES COVERED Technical Memorandum

4. TITLE AND SUBTITLE Optimal Frequency-Domain System Realization with Weighting	5. FUNDING NUMBERS WU 522-32-41-03
6. AUTHOR(S) Jer-Nan Juang and Peiman G. Maghami	

7. PERFORMING ORGANIZATION NAME(S) AND ADDRESS(ES) NASA Langley Research Center Hampton, VA 23681–2199	8. PERFORMING ORGANIZATION REPORT NUMBER L–17845

9. SPONSORING/MONITORING AGENCY NAME(S) AND ADDRESS(ES) National Aeronautics and Space Administration Washington, DC 20546–0001	10. SPONSORING/MONITORING AGENCY REPORT NUMBER NASA/TM–1999–209135

11. SUPPLEMENTARY NOTES

12a. DISTRIBUTION/AVAILABILITY STATEMENT Unclassified-Unlimited Subject Category 39 Distribution: Standard Availability: NASA CASI (301) 621–0390	12b. DISTRIBUTION CODE

13. ABSTRACT *(Maximum 200 words)*

Several approaches are presented to identify an experimental system model directly from frequency response data. The formulation uses a matrix-fraction description as the model structure. Frequency weighting such as exponential weighting is introduced to solve a weighted least-squares problem to obtain the coefficient matrices for the matrix-fraction description. A multi-variable state-space model can then be formed using the coefficient matrices of the matrix-fraction description. Three different approaches are introduced to fine-tune the model using nonlinear programming methods to minimize the desired cost function. The first method uses an eigenvalue assignment technique to reassign a subset of system poles to improve the identified model. The second method deals with the model in the real Schur or modal form, reassigns a subset of system poles, and adjusts the columns (rows) of the input (output) influence matrix using a nonlinear optimizer. The third method also optimizes a subset of poles, but the input and output influence matrices are refined at every optimization step through least-squares procedures.

14. SUBJECT TERMS System Identification, System Realization, Modal Parameter Identification, Frequency Response Function	15. NUMBER OF PAGES 48
	16. PRICE CODE A04

17. SECURITY CLASSIFICATION OF REPORT Unclassified	18. SECURITY CLASSIFICATION OF THIS PAGE Unclassified	19. SECURITY CLASSIFICATION OF ABSTRACT Unclassified	20. LIMITATION OF ABSTRACT

NSN 7540-01-280-5500

Standard Form 298 (Rev. 2-89)
Prescribed by ANSI Std. Z39-18
298-102